NOVA SCHOOL OF SCIENCE & TECHNOLOGY

DEPARTAMENT OF LIFE SCIENCES

Diana Sofia Ferreira Tavares

BSc in Biomedical Sciences

# The role of GSH signaling in mitophagy induced by reactive oxygen species: potential target for neuroprotection in stroke?

MASTER IN MOLECULAR GENETICS AND BIOMEDICINE

NOVA University Lisbon

September, 2022

NOVA SCHOOL OF SCIENCE & TECHNOLOGY

DEPARTAMENT OF LIFE SCIENCES

# The role of GSH signaling in mitophagy induced by reactive oxygen species: potential target for neuroprotection in stroke?

**DIANA SOFIA FERREIRA TAVARES**

BSc in Biomedical Sciences

**Adviser:** Helena Luísa de Araújo Vieira
*Assistant Professor, NOVA University Lisbon*

**Examination Committee:**

**Chair:** Pedro Manuel Brôa Costa, PhD
*Assistant Professor, NOVA University Lisbon*

**Rapporteurs:** Andreia Neves Carvalho, PhD
*Investigadora da Faculdade de Farmácia da Universidade de Lisboa*

**Adviser:** Helena Luísa de Araújo Vieira, PhD
*Assistant Professor, NOVA University Lisbon*

MASTER IN MOLECULAR GENETICS AND BIOMEDICINE

NOVA University Lisbon
September, 2022

**The role of GSH signaling in mitophagy induced by reactive oxygen species: potential target for neuroprotection in stroke?**

# ACKNOWLEDGMENTS

Em primeiro lugar, gostava de agradecer à minha orientadora a Dra. Helena Vieira, por me acolher no seu laboratório e me ter proporcionado a oportunidade de aprender e crescer, tanto a nível profissional como pessoal. Agradeço os ensinamentos, a gentileza, a motivação, a liberdade para aprender e errar.

Uma palavra de apreço, também, as minhas colegas de laboratório e amigas, Catarina Pires e Catarina Simões, pois sem elas não teria sido a mesma coisa, pela companhia, apoio, entreajuda e harmonia que sempre nos caracterizou.

A todos os meus amigos que ao longo do tempo se a tornaram a minha família fora de casa, por todos os momentos de convívio, almoços, jantares, idas à praia, passeios, pela leveza que trouxeram nos momentos mais complicados. Também as minhas amigas que mesmo estando longe serão sempre um porto de abrigo. Em especial, um agradecimento à Gui e à Susi, por todos os dias aturarem os meus devaneios e por terem tornado esta jornada tão mais fácil, não sei o que seria de mim sem vocês.

A toda a minha família agradeço a constante preocupação e carinho. Em especial, quero agradecer aos meus pais, por tudo, por me amarem incondicionalmente, por me apoiarem e embarcarem comigo em todas as minhas aventuras, por me fazerem sentir uma sortuda todos os dias. Obrigada, sem vocês nada seria possível, amo-vos.

A todos, um obrigada, esta tese é também um pouco vossa!

# Abstract

Mitochondria are involved in numerous cellular processes, including energy production and cell death regulation. Simultaneously, these are the main cellular producers of reactive oxygen species (ROS), particularly when dysfunctional. ROS accumulation leads to oxidative stress which is associated with pathologies, such as stroke and neurodegenerative diseases. So, elimination of ROS-producing damaged mitochondria is key for maintaining cell homeostasis. Mitophagy, consists of the selective degradation of excessive or damaged mitochondria. The accumulation of ROS and mitochondrial depolarization stimulates PTEN-induced kinase 1 (PINK1)/PARKIN-mediated mitophagy. Concomitantly, ROS are counteracted by glutathione, a key antioxidant. ROS oxidize glutathione and stimulate protein S-glutathionylation, a post-translation modification capable of modulate protein function. Here, the main goal was to explore the molecular mechanisms underlying mitophagy, in particular the role of ROS and/or glutathione signaling in mitophagy progression, with a special focus on protein S-glutathionylation. We hypothesized that mitophagy can be regulated by glutathione signaling, namely that the accumulation of mitochondrial ROS stimulates the production and oxidation of glutathione, which enhances/stimulates mitophagy by protein glutathionylation of mitophagy-related proteins. Using human cell lines, SH-SY5Y and SH-SY5Y mitoQC, mitochondrial dysfunction was stimulated with the classical uncoupler carbonyl cyanide m-chlorophenylhydrazone (CCCP). ROS generation and PINK1/PARKIN-dependent mitophagy were observed after CCCP treatment. Likewise, the catalytic subunit of the rate limiting enzyme for glutathione synthesis, Glutamate-Cysteine Ligase, is upregulated in CCCP-treated cells. Notably, we show for the first time that CCCP treatment induces protein S-glutathionylation of PINK1. Furthermore, we also found fluorescence measure on a microplate reader to be a possible new technique to assess mitophagy. Understating mitophagy mechanisms and how these are regulated is key to

stimulate cytoprotection by preventing cell death. Thus, this can eventually contribute to new strategies against diseases characterized by mitochondrial damage, like stroke.

**Keywords**: Mitochondria, Oxidative Stress, Mitophagy, Glutathione, Protein S-glutathionylation, Stroke

# RESUMO

As mitocôndrias são essenciais em processos celulares como produção de energia e regulação da morte celular. Simultaneamente, são as principais produtoras de espécies reativas de oxigênio (ROS), particularmente quando disfuncionais. A acumulação de ROS leva a stress oxidativo que está associado a patologias, como acidente vascular cerebral e doenças neurodegenerativas. Assim, a eliminação de mitocôndrias danificadas produtoras de ROS é fundamental para a homeostase celular. A mitofagia consiste na degradação seletiva de mitocôndrias excessivas ou danificadas. Acumulação de ROS e despolarização mitocondrial estimulam mitofagia via quinase 1 induzida por PTEN (PINK1)/PARKIN. Concomitantemente, ROS são neutralizados pela glutationa, um antioxidante chave. As ROS oxidam a glutationa e estimulam s-glutationilização, uma modificação pós-traducional capaz de modular a função proteica. Aqui, o objetivo foi explorar os mecanismos subjacentes à mitofagia, particularmente o papel da sinalização de ROS e/ou glutationa na progressão da mitofagia, com foco especial na s-glutationilização. Colocamos a hipótese que a mitofagia pode ser regulada pela sinalização da glutationa, nomeadamente que a acumulação de ROS mitocondriais estimula a produção e oxidação de glutationa, que estimula a mitofagia por S-glutationilização de proteínas relacionadas com mitofagia. Em linhas celulares humanas, SH-SY5Y e SH-SY5Y mitoQC, disfunção mitocondrial foi estimulada com *carbonyl cyanide m-chlorophenylhydrazone* (CCCP). Geração de ROS e mitofagia dependente de PINK1/PARKIN foram observados após tratamento com CCCP. Igualmente, a subunidade catalítica da enzima limitante da síntese de glutationa, Glutamato-Cisteína Ligase, é sobre-expressa em células tratadas com CCCP. Notavelmente, mostramos que tratamento com CCCP induz glutationilização de PINK1. Além disso, também descobrimos que medir fluorescência num leitor de microplacas é uma possível técnica para avaliar mitofagia. Compreender os mecanismos de mitofagia e como são regulados é fundamental para estimular a citoproteção prevenindo a morte celular. E eventualmente contribuir para

novas estratégias contra doenças caracterizadas por danos mitocondriais, como o acidente vascular cerebral.

**Palavras chave:** Mitocôndrias, Stress oxidativo, Mitofagia, Glutationa, S-glutationilização proteica, acidente vascular cerebral.

# CONTENTS

# LIST OF FIGURES

# LIST OF TABLES

# LIST OF ABBREVIATIONS, ACRONYMS AND CHEMICAL SYMBOLS

| | |
|---|---|
| **ATP** | Adenosine triphosphate |
| **BCA** | Bicinchoninic acid |
| **BNIP3** | Bcl-2 19-kDa interacting protein 3 |
| **BSA** | Bovine serum albumin |
| **$Ca^{2+}$** | Calcium cation |
| **CCCP** | Carbonyl cyanide m-chlorophenylhydrazone |
| **CK2** | Casein kinase 2 |
| **DCF** | 2',7'-dichlorofluorescein |
| **DMEM -F12** | Dulbecco's Modified Eagle Medium: Nutrient Mixture F-12 |
| **DMSO** | Dimethyl Sulfoxide |
| **DNA** | Deoxyribonucleic acid |
| **DTNB** | 5,5-dithio-bis-(2-nitrobenzoic acid) |
| **Drp1** | Dynamin related protein 1 |
| **ECL** | Enhanced chemiluminescence |
| **EDTA** | Ethylenediaminetetraacetic acid |
| **ERRs** | Estrogen related receptors |
| **$FADH_2$** | Flavin adenine dinucleotide |

| | |
|---|---|
| **FBS** | Fetal Bovine Serum |
| **FIS1** | Mitochondrial fission 1 protein |
| **FUNDC1** | FUN14 domain-containing protein 1 |
| **GCL** | Glutamate-cysteine ligase |
| **GCLC** | Glutamate-cysteine ligase catalytic subunit |
| **GCLM** | Glutamate-cysteine ligase modulatory subunit |
| **GFP** | Green fluorescence protein |
| **GGT** | Glutamyltranspeptidase |
| **GPX** | Glutathione peroxidases |
| **GR** | Glutathione reductase |
| **GRX** | Glutaredoxin |
| **GS** | Glutathione synthetase |
| **GSH** | Reduced glutathione |
| **GSSG** | Oxidized glutathione |
| **$H^+$** | Hydrogen cation |
| **$H_2$DCFDA** | 2′,7′ dichlorofluorescein diacetate |
| **$H_2O$** | Water |
| **$H_2O_2$** | Hydrogen peroxide |
| **HCL** | Hydrogen chloride |
| **HIF** | α1- Hypoxia-Inducible Factor-1α |
| **IMM** | Inner mitochondrial membrane |
| **$K_2HPO_4$** | Dipotassium Phosphate |
| **$KH_2PO_4$** | Potassium dihydrogen phosphate |
| **KCl** | Potassium Chloride |
| **LB** | Loading buffer |
| **LC3** | Microtubule |
| **LIR** | Microtubule-associated protein 1A/1B-light chain 3 |
| **Mff** | Mitochondrial fission factor |
| **MgCl2** | Magnesium chloride |
| **MiD49** | Mitochondrial dynamics proteins 49 |

| | |
|---|---|
| **MiD51** | Mitochondrial dynamics proteins 51 |
| **MPP** | Matrix processing peptidase |
| **MPTP** | Mitochondrial permeability transition pore |
| **MQC** | Mitochondrial quality control |
| **Mtf** | Mitofusins |
| **MTS** | Mitochondrial targeting sequence |
| **$Na^+$** | Sodium cation |
| **$Na_2HPO_4$** | disodium hydrogen phosphate |
| **NaCl** | Sodium chloride |
| **NADH** | Nicotinamide adenine dinucleotide |
| **NADPH** | Nicotinamide Adenine Dinucleotide Phosphate |
| **Nf-kB** | Nuclear factor kappa B |
| **NIX** | BCL2 interacting protein 3 |
| **NRF1** | Nuclear respiratory factor 1 |
| **NRF2** | Nuclear respiratory factor 2 |
| **NRF2L2** | Nuclear factor erythroid 2 related factor 2 |
| **$O_2$** | Oxygen |
| **$O_2^{\bullet-}$** | Anion superoxide |
| **$OH^{\bullet}$** | Hydroxyl radical |
| **OPA1** | Optic Atrophy Protein 1 |
| **OXPHOS** | Oxidative phosphorylation |
| **PARL** | Presenilin associated rhomboid |
| **PBS** | Phosphate buffered saline |
| **PFA** | Paraformaldehyde |
| **PGAM5** | PGAM Family Member 5 |
| **P-Glu** | Protein S-glutathionylation |
| **PINK1** | PTEN- induced putative kinase 1 |
| **RIPA** | Radioimmunoprecipitation assay buffer |
| **RNA** | Ribonucleic acid |
| **RNS** | Nitrogen reactive species |

| | |
|---|---|
| **ROS** | Reactive oxygen species |
| **RT** | Room temperature |
| **SDS** | Sodium dodecyl sulfate |
| **siRNA** | small interfering RNA |
| **SDHA** | Succinate dehydrogenase complex, subunit A |
| **SOD** | Superoxide dismutase |
| **t-BHP** | Tert- butylhydroperoxide |
| **TEMED** | Tetramethylethylenediamine |
| **TIM** | Inner membrane translocase |
| **TNB** | 5-thio-2-nitrobenzoic acid |
| **TOM** | Outer membrane translocase |
| **Tris-HCL** | Tris(hydroxymethyl)aminomethane hydrochloride |
| **T-TBS** | tert-Butyldimethylsilyl chloride |
| **ULK1** | Unc-51 Like Autophagy Activating Kinase 1 |

# 1

# INTRODUCTION

## 1.1 Ischemic stroke

Stroke is a life-threatening medical condition that is characterize by the loss of blood flow in the central nervous system, being a major cause of brain injury, neuronal disability, and death worldwide[1]. Stroke can be hemorrhagic or ischemic[2–4]. Ischemic stroke happens when a clot occludes a blood vessel preventing normal blood flow into the brain and accounts for 85% of stroke cases[4]. The other 15% corresponds to hemorrhagic stroke that occurs when a blood vessel bursts causing either an intracerebral or subarachnoid hemorrhage[4,5].

The brain is a highly demanding organ in glucose and oxygen ($O_2$), thus it is particularly susceptible to damage by stroke, such that irreversible damage can occur only 30 minutes after ischemia[6]. When blood flow is interrupted, cells enter into hypoxia and energy failure. Adenosine triphosphate (ATP) shortage leads to anaerobic glycolysis activation, cell depolarization and glutamate release into the extracellular space causing excitotoxity. Consequently, membrane ion exchange and transporters activity is altered leading to the accumulation of $H^+$, $Na^+$ and $Ca^{2+}$ in the cytosol, causing organelle and cell swelling. Furthermore, $Ca^{2+}$ overload leads to mitochondrial damage, with activation of proteases, lipases and endonucleases, which boosts the production of reactive oxygen species (ROS) leading to oxidative stress, disruption of cellular structures and finally induction of cell death [4,7,8] .Therefore, to avoid tissue damage and permanent lesion, it is critical to reestablish the blood flow (reperfusion) as soon as possible.

The cells primarily irrigated by the infarcted vessel have their blood flow drop to 10-25% of basal level, consequently these cells are almost immediately compromised and die rapidly

by necrosis, forming the ischemic core (Figure 1.1) [4,9,10]. On the other hand, the cells surrounding the ischemic core still sustain some perfusion provided by collateral vessels, these suffer from milder damage and constitute the penumbra area (Figure 1.1) [11,12]. Even though, these cells are damage, they are still viable[4]. Penumbra cells are subjected to delayed inflammation and cell death mainly by apoptosis, which progressively aggravates the ischemic lesion[9]. Accordingly, these cells can still be salvageable and regain normal function if a rapid therapeutic response is initiated and perfusion is reestablished. Therefore, penumbra cells are the main target for ischemic stroke potential treatment [4].

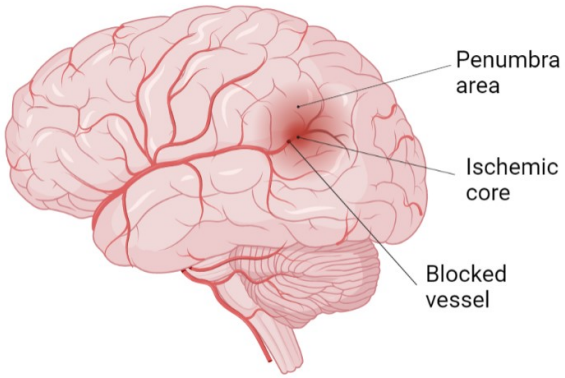


Figure 1.1 — **Ischemic stroke illustration**. The cells directly irrigated by the blocked vessel and that have perfusion values bellow viability, die almost immediately and form the ischemic core. The cells that surround this core and still sustain perfusion levels to remain viable form the penumbra area, these cells are subjected to delayed inflammation and cell death by apoptosis, which progressively aggravates the ischemic lesion. Created with BioRender.com.

The longer the ischemic period, the worse the outcome. To date, the available treatments for ischemic stroke are based on the re-establishment of blood flow (reperfusion), these consist of administration of thrombolytic agents or mechanical endovascular thrombectomy. However, treatment effectiveness has a limited time window and not all patients are suited for treatment [13,14].

Reperfusion is vital to maintain tissue viability and to allow penumbra area cells to recover[11]. Nevertheless, it is also associated with oxidative stress and tissue damage occurring during blood reperfusion[7] . This damage generated by the reoxygenation of the tissues flowing reperfusion is known as ischemic/reperfusion lesion[15]. Once the blood flow is reestablished and $O_2$ is again available, mitochondrial aerobic respiration is reactivated, and there is a burst of ROS generation by the hyperactivity of mitochondria and pro-oxidant enzymes (like xanthine oxidase and NADPH oxidase) [16,17]. These ROS overpower weakened antioxidant defenses

leading to harmful signaling cascades and oxidative stress that causes the opening of the mitochondrial permeability transition pore (MPTP), which causes the loss of mitochondrial potential and consequently of energy production. This is followed by mitochondrial fragmentation and release of mitochondrial pro-apoptotic factors that culminates in the activation of apoptosis and further extent of the brain injury[7,18].

Mitochondria are key regulators of cell fate, being involved in both apoptosis and necrosis, the two main cellular death pathways. Thus, it is essential that these organelles remain functional, and whenever a dysfunctional abnormality occurs, they must be eliminated. Mitophagy or selective mitochondrial autophagy is the cellular process to eliminate dysfunctional mitochondria. Mitophagy has already been described as a cytoprotective mechanism during ischemia/reperfusion lesion, as it limits the induction of cell death via damage mitochondria [19]. Hence, it is important to explore mitophagy induction and regulation, and how it can contribute to better outcomes in neuronal diseases such as stoke.

## 1.2 Mitochondria and ROS

Mitochondria are double-membrane intracellular organelles that are vital for several processes in the cell, including metabolism modulation and cell death control[20]. Mitochondrial primary function is the generation of ATP through oxidative phosphorylation (OXPHOS), although other metabolic processes occur, namely beta-oxidation[21], heme biogenesis[22], Fe-S clusters generation[23], calcium storage among others[20].

During OXPHOS, electrons donated by nicotinamide adenine dinucleotide (NADH) and flavin adenine dinucleotide ($FADH_2$) are transferred along respiratory complexes to reduce $O_2$ into water ($H_2O$). These respiratory complexes make up the electron respiratory chain in the inner mitochondrial membrane (IMM) and consist of complex I (NADH dehydrogenase (ubiquinone), complex II (succinate dehydrogenase), complex III (ubiquinol-cytochrome c reductase) and complex IV (cytochrome c oxidase). During this process $H^+$ ions are pumped across the IMM into the intermembrane space generating a membrane potential between the matrix and the intermembrane space. This allows the generation of ATP by ATP synthase (Complex V)[24] as the protons diffuse back into the matrix in the last step of the chain (Figure 1.2).

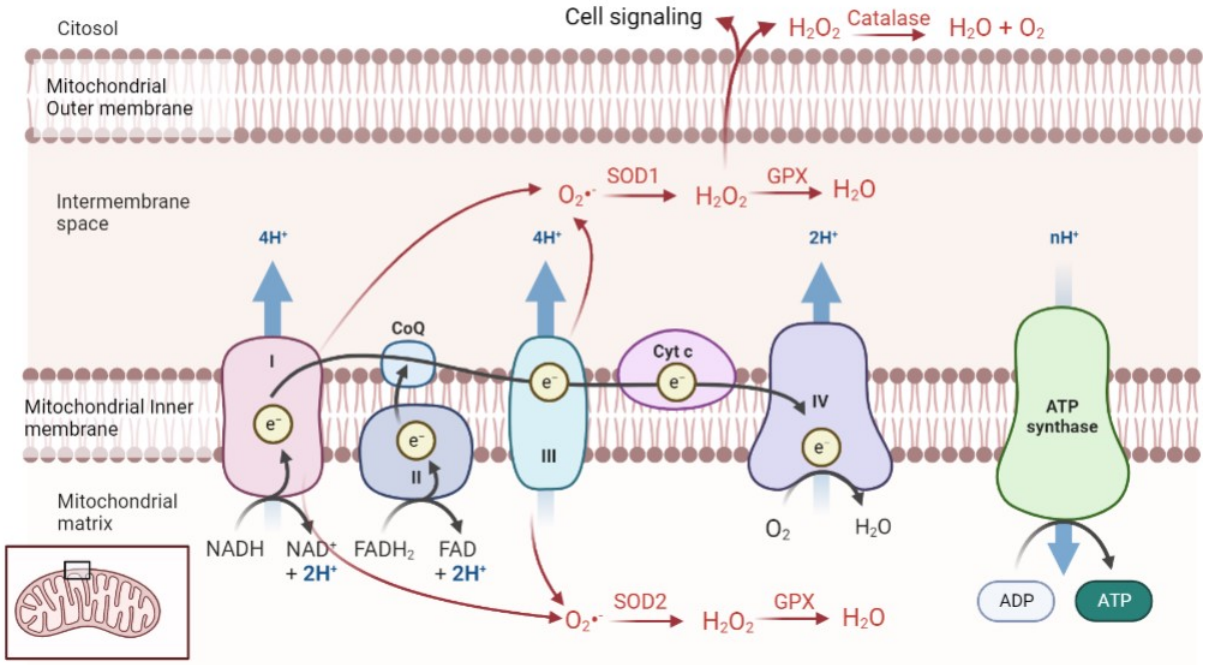


Figure 1.2 **Oxidative phosphorylation and reactive oxygen species production**. During oxidative phosphorylation electrons ($e^-$) donated by nicotinamide adenine dinucleotide (NADH) and flavin adenine dinucleotide (FADH2) are transferred along the complexes that make up the electron respiratory chain to reduce oxygen ($O_2$) into water ($H_2O$). During this process, electrons leak and generate ion superoxide (O2•−) that is rapidly dismutated into hydrogen peroxide ($H_2O_2$) by superoxide dismutase (SOD) 1 and 2. By its turn, $H_2O_2$ can be reduced by several enzymes, which include glutathione peroxidases (GPX) and peroxiredoxins (whose actions are dependent on the reducing potential of NADPH) and the cytosolic catalase which catabolizes $H_2O_2$ in $H_2O$ and $O_2$. Still some $H_2O_2$ escapes and acts as signaling molecule in cellular processes like proliferation and differentiation. Created with BioRender.com. Adapted from [25]

During this process some of the electrons can leak, mainly through complexes I and III [26]. These leaked electrons react with $O_2$ to form anion superoxide ($O_2^{\bullet-}$), which can then react to originate other ROS, such as $H_2O_2$ and hydroxyl radical ($OH^{\bullet}$), making the mitochondria the main source ROS in the cells[26]. In fact, under normal physiological conditions, 1-2% of $O_2$ is not totally reduced into $H_2O$, forming $O_2$•− [26] (Figure 1.2). This basal ROS formation is involved in signaling processes, participating in the cellular homeostasis and metabolic regulation.

In fact, at low doses, ROS have an important role working as signaling molecules[20]. In particular, $H_2O_2$ is the main signaling molecule since it is stable and diffuses out of the mitochondria, modulating transcription factors and other proteins, which in turn controls cellular processes such as cell proliferation[27], differentiation [28] and survival[29] .

Excessive levels of ROS are counteracted by antioxidants systems and enzymes. In this case, mitochondrial superoxide dismutase (SOD) 1 in the mitochondria intermembrane space and SOD 2 in the mitochondrial matrix act to dismutate $O_2^{\bullet-}$ into $H_2O_2$ and $O_2$. By its turn, $H_2O_2$

can be reduced by several enzymes, which include glutathione peroxidases (GPX) and peroxiredoxins (whose actions are dependent on the reducing potential of NADPH) and the cytosolic catalase which catabolizes $H_2O_2$ into $H_2O$ and $O_2$ [26] (Figure 1.2).

Whenever ROS accumulate, due to their overproduction or insufficient antioxidant defenses, they become deleterious. High levels of ROS generate oxidative stress, that affects several cellular components, including DNA, lipids, and proteins and are associated with several diseases such as cancer, neurodegenerative and autoimmune diseases[24]. As oxidative damage increases, mitochondria can become dysfunctional, generating more ROS into an amplification loop, which can lead to cellular stress and eventually cell death. Thus, mitochondrial ROS production and their elimination must be tightly controlled. For this and to keep cellular homeostasis, mitochondrial quality control (MQC) systems are essential and work in a fine-tuned coordination[30].

## 1.3 Mitochondrial quality control (MQC)

Mitochondria are dynamic organelles that undergo several processes to keep cell homeostasis and energy demand. Since mitochondria control metabolism, cell fate and ROS production, several MQC mechanisms must exist to maintain a healthy mitochondrial population. MQC includes various processes, namely: mitochondrial fusion/fission, mitochondrial biogenesis and mitophagy[31,32]. Mitophagy is the most prominent process associated with MQC and will be reviewed in more detail later in this introduction.

**Mitochondrial biogenesis** is the process by which new mitochondria are generated from preexisting ones[33,34]. This process is essential to maintain a healthy mitochondrial population and to meet cellular energy demand. Mitochondrial biogenesis is induced in response to environmental signals and under conditions of stress and energy requirement like physical exercise[35], cold exposure[36] or hypoxia[37,38]. This process is regulated by peroxisome proliferator-activated receptor gamma coactivator 1a (PGC-1a) protein [39], which activates transcription factors including Nuclear respiratory factor 1 (NRF1), Nuclear respiratory factor 2 (NRF2), and estrogen related receptors (ERRs). NRF1, NRF2 and ERR are important transcription factors that promote

the transcription of mitochondrial and nuclear-encoded mitochondrial genes, in a coordinated fashion for the correct mitochondrial biogenesis[40,41].

**Fusion and fission** are opposite mechanisms that work in balanced dynamic transitions to respond to physiological and metabolic cellular needs. When kept in equilibrium, these processes allow the maintenance of an adequate mitochondrial population, with the right number, size, shape, and function.[32]

Fission is controlled by the interaction of the GTPase dynamin related protein 1 (Drp1) with mitochondrial receptors, namely mitochondrial fission protein 1 (Fis1), mitochondrial fission factor (Mff), and mitochondrial dynamics proteins 49 and 51 (MiD49, MiD51) [32]. Drp1 accumulates in the OMM in a ring like structure and triggers the cleavage of the mitochondria into two by constriction. Fission allows the uneven distribution of mitochondrial components within the two new daughter mitochondria, thereby it can generate one healthy mitochondrion that is maintained and a damaged/dysfunctional one suitable for elimination. Hence, fission is indispensable to keep a heathy mitochondrial pool[42]. Notably, fission is also crucial for an effective mitophagy, as it reduces the size of mitochondria for the autophagosome engulfment [43] (Figure 1.3).

One the other hand, the process of fusion combines two or more mitochondria into one, and can be an attempt to recover partially damaged mitochondria. Fusion allows the junction between mitochondria with differently damaged components that when combine balance each other enabling mitochondrial potential maintenance and avoiding oxidative damage[44,45]. This process is dependent on the GTPases optic atrophy protein 1 (OPA1) and mitofusins (Mtf) 1 and 2. Upon stimulation, Mtf 1 and 2 ,that are present on the OMM of the two adjacent mitochondria, mediate the tethering and docking of the mitochondria allowing the fusion of the OMMs, whereas OPA1 proceeds the fusion between the IMMs, forming one new elongated mitochondrion[46] (Figure 1.3).

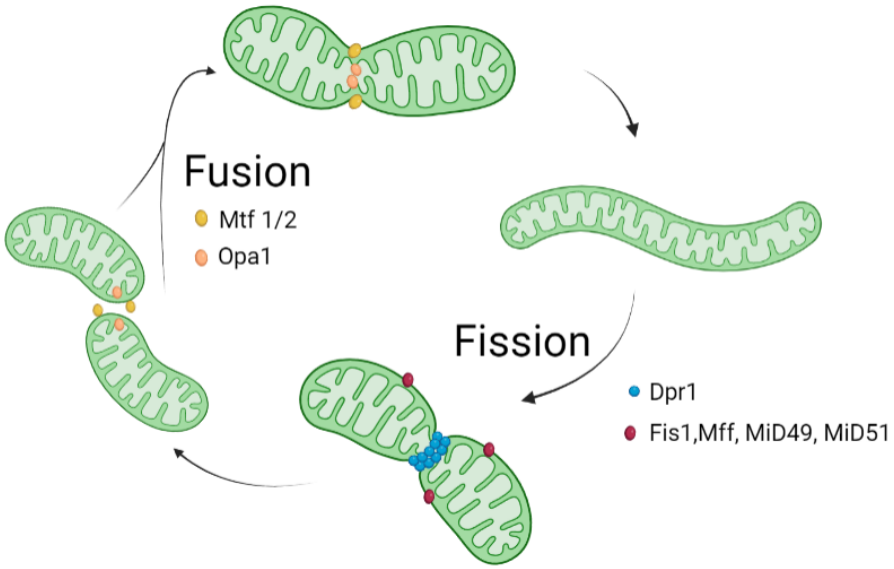


Figure 1.3 **Mitochondrial fission and fusion**. Mitochondria are dynamic organelles that can adapt to the environment. Fission and fusion are balanced opposite mechanisms that maintain a healthy mitochondrial population. Fission allows the fragmentation of mitochondria and the uneven distribution of mitochondrial components within the two new daughter mitochondria. Fission is controlled by the interaction of the GTPase dynamin related protein 1 (Drp1) with mitochondrial receptors, namely mitochondrial fission protein 1 (Fis1), mitochondrial fission factor (Mff), and mitochondrial dynamics proteins 49 and 51 (MiD49, MiD51). Drp1 accumulates in the OMM in a ring like structure and triggers the cleavage of the mitochondria into two by constriction. One the other hand, the process of fusion combines two or more mitochondria into one. This process is dependent on the GTPases optic atrophy protein 1 (OPA1) and mitofusins (Mtf) 1 and 2. Upon stimulation, Mtf 1 and 2 on the OMM of the two adjacent mitochondria, mediate the tethering and docking of the mitochondria allowing the fusion of the OMMs, whereas OPA1 proceeds the fusion between the IMMs, forming one new elongated mitochondrion. Created with BioRender.com, adapted from [47].

## 1.4 Autophagy

Autophagy is a multistep process essential to keep cell homeostasis that culminates in the digestion and recycling of impaired cellular components in the lysosomes[48,49]. It is triggered in response to several stimuli, namely misfolded proteins, protein aggregates, damaged organelles, or nutrient starvation[50]. Thus, autophagy is an essential process to keep energy balance and cell homeostasis[50].

There are three types of autophagy that mainly differ in the method of cargo capture: Chaperone-mediated autophagy (CMA), in which specific target proteins form a complex with chaperon proteins that are recognized by lysosomes. Microautophagy, where cytosolic components are engulfed directly by lysosomes. Finally, macroautophagy (normally known as autophagy), where cargo is captured by a double membrane vesicle known as phagophore to

form the autophagosome, that later fuses with the lysosome to form the autolysosome, where the cargo is degraded by the proteases and other lysosomal digestive enzymes. The digested material is then reused to form new cellular components[51,52].

Autophagy can also be classified as selective or non-selective. In non-selective autophagy cargo is collected from the cytosol in bulk and is delivered into the lysosomes. Usually, non-selective autophagy is induced by starvation state. Selective autophagy occurs under a constitutive manner and is dependent on specific cargo receptors. Selective autophagy can specifically target microorganisms, excessive or impaired organelles or proteins. Considering the type of cargo, selective autophagy can be subdivided into several types such as mitophagy, nucleophagy, glycophagy, lipophagy whose targets are mitochondria, the nucleus, glycogen, and lipids, respectively.[49]

## 1.5 Mitophagy

Mitophagy consists in the selective degradation of damaged or excessive mitochondria[30]. Mitophagy is an essential process for MQC and to keep mitochondrial and cellular homeostasis. Usually, mitophagy is a cytoprotective and adaptative mechanism, however when uncontrolled it can lead to ATP shortage and represent a threat to the cells[53]. In fact, defects in the mitophagic process have been associated with ageing and several neurologic pathologies like Parkinson's disease[54] and Alzheimer's disease [55].

Functionally mitophagy can be: (i) basal, to maintain a normal mitochondrial population and ensure the removal of aged mitochondria; (ii) programmed, to remove mitochondria during cell development and differentiation or (iii) stress-induced, occurring in response to different stimuli/stresses[56,57]. There are three main identified pathways by which mitophagy can occur, these pathways can be divided into ubiquitin-dependent and ubiquitin-independent pathways.

## 1.5.1 Ubiquitin-dependent pathways:

### 1.5.1.1 PINK1/PARKIN pathway

PTEN-induced putative kinase 1 (PINK1)/PARKIN pathway is one of the most studied and described pathways, mainly due to the fact that these proteins mutation is connected to autosomal recessive forms of Parkinson's disease[58]. It is a Ubiquitin-dependent pathway and is stress associated. For example, this pathway was shown to be engaged by cerebral ischemia and reperfusion[59]. PINK1 is a nucleus-encoded mitochondrial kinase that is constitutively expressed, and PARKIN is a cytosolic E3-ubiquitin ligase that functions downstream of PINK1[60].

In healthy mitochondria, the full length PINK1 (63kDa) is imported from the cytosol to the mitochondria through the translocase outer membrane (TOM) and translocase inner membrane (TIM) complexes due to PINK1's mitochondrial targeting sequence (MTS). In the mitochondrial matrix, PINK1 is cleaved by matrix processing peptidase (MPP) and then, in the inner membrane by presenilin associated rhomboid-like protein (PARL)[61,62]. The unstable cleaved form of PINK1 (52kDa) is then returned to the cytosol where it is degraded by the ubiquitin-proteasome system[63] (Figure 1.4).

In damaged mitochondria, the loss of mitochondrial membrane potential impairs PINK1 import to the IMM, making it unreachable by PARL and MPP. Consequently, full length PINK1 stabilizes and accumulates into the OMM in a complex with TOM proteins[64]. In the OMM, PINK1 dimerizes and auto-phosphorylates in Ser-228 and Ser-402 becoming activated[65,66]. Activated PINK1 phosphorylates ubiquitin linked to OMM proteins and pre-existing ubiquitin in the OMM. This recruits PARKIN, that recognizes the phosphorylated domains[67]. In the OMM, PARKIN is phosphorylated in its ubiquitin like domain (Ser65) and activated by PINK1[67–69]. Activated PARKIN polyubiquitinates proteins, such as Mitofusins 1 and 2[70], and VDAC1[71] in the outer membrane[72]. These ubiquitin chains are recognized by ubiquitin-binding cargo receptors, namely optineurin[73] and p62[71], which in turn are recognized by autophagosome membrane microtubule-associated protein 1A/1B-light chain 3 (LC3) proteins due to their LC3-interacting region (LIR) motifs, targeting mitochondria for digestion (Figure 1.4).

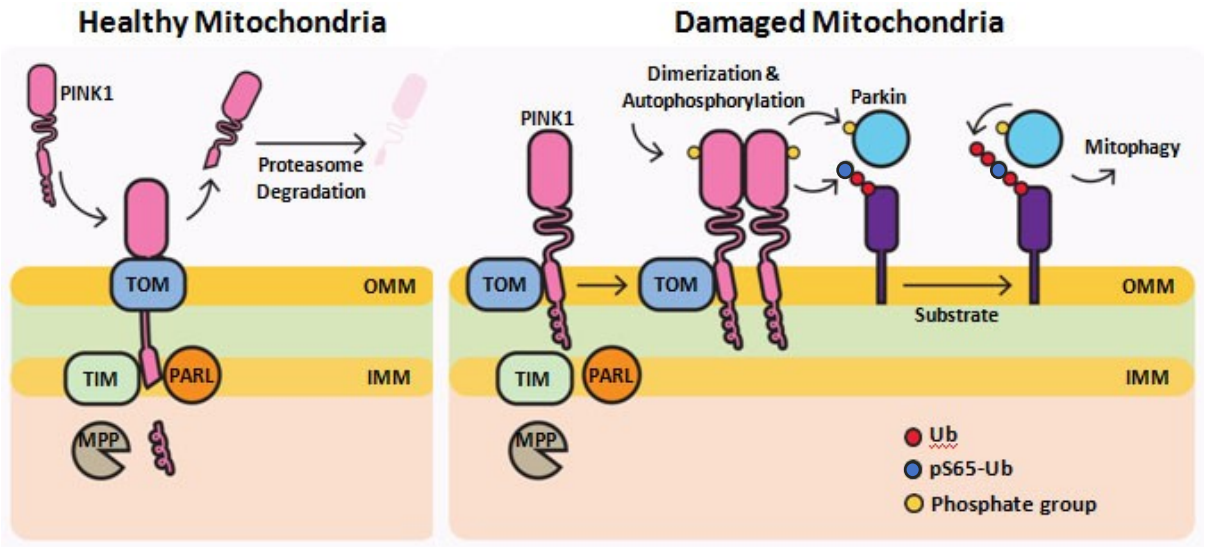


Figure 1.4 **PINK1/PARKIN mediated mitophagy.** In healthy mitochondria, the full length PINK1 (63kDa) is imported from the cytosol to the mitochondria through the translocase outer membrane (TOM) and translocase inner membrane (TIM) complexes. In the mitochondrial matrix, PINK1 is cleaved by matrix processing peptidase (MPP) and then, in the inner membrane by presenilin associated rhomboid-like protein (PARL). The unstable cleaved form of PINK1 (52kDa) is then returned to the cytosol where it is degraded by the ubiquitin-proteasome system. In damaged mitochondria, the loss of mitochondrial membrane potential impairs PINK1 traffic/import to the IMM, making it unreachable by the proteases. Consequently, full length PINK1 stabilizes and accumulates in the OMM in a complex with TOM proteins. In the OMM, PINK1 dimerizes and auto-phosphorylates becoming activated. Activated PINK1 phosphorylates pre-existing ubiquitin in the OMM, which recruits PARKIN, that is then phosphorylated and activated by PINK1. Activated PARKIN polyubiquitinates proteins in the outer membrane. These ubiquitin chains are recognized by ubiquitin-binding cargo receptors which in turn are recognized by autophagosome membrane microtubule-associated protein 1A/1B-light chain 3 (LC3) proteins targeting mitochondria for digestion. Adapted from [74] .

PINK1/PARKIN mitophagy pathway can be stimulated using different compounds. One of the most used ones is the mitochondrial uncoupler carbonyl cyanide m-chlorophenylhydrazone (CCCP)[75]. CCCP is an ionophore of hydrogen, it transports protons across the IMM which disrupts mitochondrial membrane potential, thus stimulates PINK1 accumulation in the OMM and mitophagy triggering[76].

## 1.5.2 Ubiquitin independent pathways / receptor mediated mitophagy

Some specific OMM proteins contain LIR motifs that are mitophagy receptors [77]. Depending on their phosphorylation state, these proteins are able to bind directly to LC3 proteins in the autophagosome, inducing ubiquitin independent mitophagy. These pathways can be induced either in a programmed manner or in response to stress [56] .

#### 1.5.2.1 FUNDC1 pathway

Under normal conditions, FUN14 domain-containing protein 1 (FUNDC1) is phosphorylated by casein-kinase 2 (CK2) and Src kinases, which prevents its interaction with LC3 and, therefore, the induction of mitophagy[78]. Under stress conditions, for example as hypoxia[79], FUNDC1 is dephosphorylated by PGAM Family Member 5 (PGAM5), which enables its interaction with LC3 proteins thus promoting mitophagy[78].This interaction is further enhanced by the phosphorylation of Ser17 of FUNDC1 by Unc-51 Like Autophagy Activating Kinase 1 (ULK1)[80].

#### 1.5.2.2 BNIP3 and NIX pathways

BNIP3 and NIX are members of the Bcl-2 family and have 56% similarity between each other[81]. These proteins are associated with hypoxia-induced mitophagy. The hypoxic environment stimulates the activity of the transcription factor Hypoxia-Inducible Factor-1α (HIF-α1), which promotes the overexpression of BNIP3 and NIX[30,82]. Due to the stress signals generated by hypoxia, BNIP3 and NIX protein stabilize in the OMM, where are phosphorylated by ULK1 and become capable of interacting with LC3 and promote mitophagy. Moreover, under physiological conditions, NIX also mediates mitochondrial clearance during red blood cells differentiation and maturation, in which mitophagy is an important process to eliminate mitochondria and complete their specialization [83].

In the last years several studies were conducted in an effort to better understand mitophagy and its triggers. It was found that ROS act as a trigger of PINK1/PARKIN-dependent mitophagy by inducing translocation of PARKIN to mitochondria and PINK1 stabilization on the OMM[75]. Based on this premise and on previous work from the lab using primary mice astrocytes, this is the pathway that will be focused on this work.

## 1.6 Antioxidant defenses: glutathione

Cells are constantly bombarded with stresses of endogenous and exogenous origins. In order to cope with stress, particularly oxidative stress, cells have a battery of enzymes and antioxidant molecules ready to keep oxidant levels low [84]. These molecules include reduced glutathione (GSH), one of the most important non-protein thiol molecule in the cells [85] and the

main cellular non-enzymatic anti-oxidant molecule. Antioxidants such as glutathione are key for the regulation of redox signaling pathways [86].

GSH or γ-glutamyl-cysteinyl-glycine is a tripeptide molecule, constituted by glutamate, cysteine, and glycine (Figure 1.5), existing in nearly every cell with concentrations that vary between 1-10mM [87]. GSH is pivotal for a normal antioxidant response and for the maintenance of the cellular redox state[88,89,90]. In addition to its function as an antioxidant defense, GSH is also important for numerous other functions such as cellular storage of cysteine[91] , detoxification of xenobiotics [92], biogenesis of iron clusters[93], cell cycle progression[94], cell death regulation and redox signaling.[95]

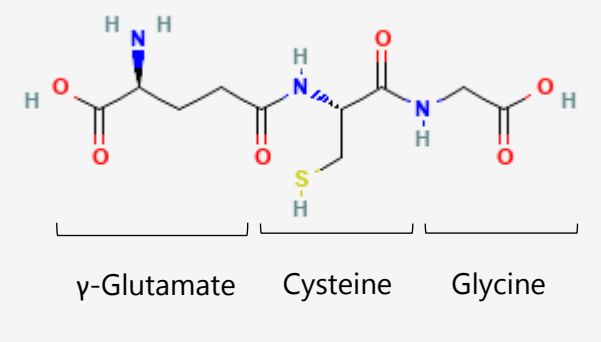


Figure 1.5 **Reduced Glutathione (GSH) chemical structure.** Adapted from PubChem

The levels of GSH in the cells depend on an equilibrium between its synthesis, utilization, export, recycling and degradation rates.

## 1.6.1 GSH synthesis

GSH is synthesized *de novo* exclusively in the cytosol, in two successive steps, and in an ATP dependent manner[95]. First, glutamate-cysteine ligase (GCL) catalyzes the formation of a γ-peptide bond between glutamate and cysteine, resulting in γ-glutamylcysteine. Next, a glycine is added to γ-glutamylcysteine by glutathione synthetase (GS) originating GSH[88,90,96] (Figure 1.6).

The rate limiting enzyme for GSH synthesis is GCL[95]. This enzyme is composed of two subunits: (i) a catalytic subunit, GCLC, responsible for catalyzing the formation of γ-glutamylcysteine from glutamate and cysteine, and (ii) a modulatory subunit, GCLM, which regulates the kinetics of the holoenzyme increasing the efficiency of γ-glutamylcysteine formation[97]. These subunits are subjected to regulation by transcription factors that include the master

regulator of antioxidant response, nuclear factor-erythroid 2 related factor 2 (NRF2L2), which is sensitive to oxidative stress and activates antioxidant responses. [90,98] Other regulators include nuclear factor kappa B (Nf-kB) [98] and activator protein-1 (AP1)[99]. The production of GSH is also influenced by other aspects such as cysteine avaibility,[89] feedback inhibition of GCL by GSH[100] and ATP availability [90].

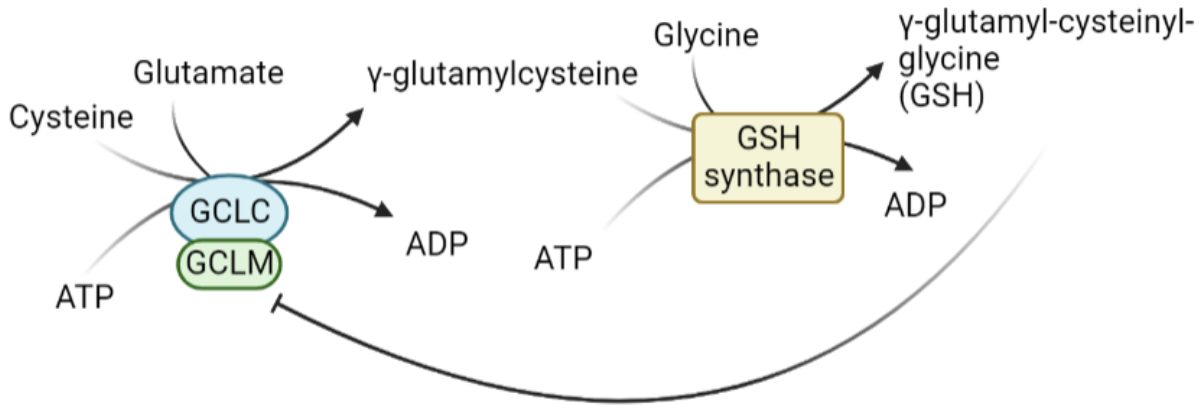


Figure 1.6 **Glutathione synthesis**. Glutamate-cysteine ligase (GCL) catalyzes the formation of a γ-peptide bond between glutamate and cysteine, resulting in γ-glutamylcysteine. Next, a glycine is added to γ-glutamylcysteine by glutathione synthetase (GS) originating GSH. Both of the reactions are ATP dependent and GCL action is rate-limiting for GSH synthesis.

## 1.6.2 GSH utilization

From the cytosol, some of the GSH is then distributed to mitochondria, endoplasmic reticulum, and nucleus[101]. This allows for each compartment to have different redox pools which are adjusted to perform particular functions [101]. Mitochondrial GSH is particularly important to avoid mitochondrial oxidative damage, such as mitochondrial DNA oxidation and lipid peroxidation, as mitochondria are constantly producing ROS. In fact, it is estimated that $O_2^{\bullet-}$ levels within mitochondria are 5 to 10-fold higher than in the cytosol[102]. Therefore, GSH and GSH-dependent enzymes are essential to detoxify from ROS and other reactive species, maintaining healthy and functional mitochondria[103].

Glutathione's high concentrations (1-10mM) and low redox potential (E'0 = −240 mV) makes it an ideal cellular redox buffer[87]. The reductive power of glutathione comes from the thiol group of cysteine that donates electrons to target molecules (EX. ROS or electrophile)[89]. When GSH reacts with a ROS, two GSH molecules are oxidized to neutralize It which originates

one oxidized glutathione (GSSG) (two GSH molecules bonded by a disulfide bond). Thus, Glutathione can occur in two major forms: reduced glutathione, GSH, and oxidized glutathione, GSSG (Figure 1.7).

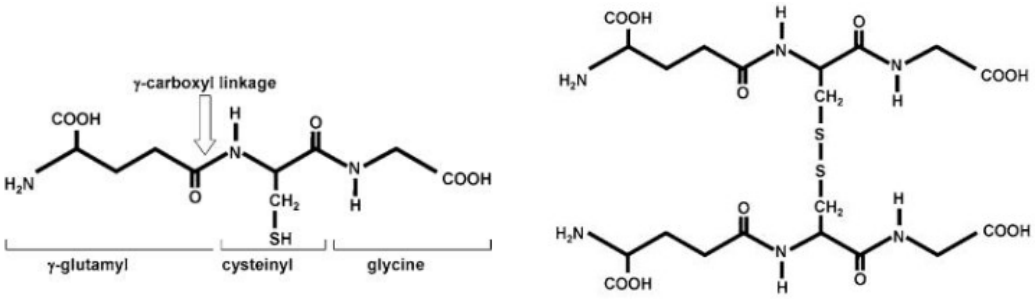


Reduced Glutathione (GSH) Oxidized Glutathione (GSSG)

Figure 1.7 **Glutathione forms**. Glutathione can occur in two major forms: reduced thiol form, GSH, and disulfide-oxidized form, GSSG. Adapted from [104]

Besides, directly react with and scavenger oxygen and nitrogen reactive species, GSH can also form mixed disulfide bonds with cysteine group of proteins. Additionally, GSH can act indirectly as a cofactor for several GSH-dependent detoxifying enzymes such as GPX, glutaredoxins (GRXs) and glutathione s-transferases [100].

## 1.6.3 Recycling, export and degradation of glutathione

For maintaining a high GSH/GSSG ratio and thus the antioxidant capabilities of the cells, GSSG can then be transformed back to GSH in a NADPH dependent way by glutathione reductase (GR)[96], or its excess can be actively exported out of the cells[104,105]. The ratio of GSH to GSSG in cells is a way to predict the oxidative state of the cells and different cell compartments have differential ratios for example, cytosolic ratio is about 100:1 and mitochondrial is about 10:1. [104]

The maintenance of the GSH/GSSG ratio homeostasis is critical for supporting a healthy redox environment and preventing oxidative stress, cellular damage, loss of function and disease onset. Changes in this ratio can severely affect cellular behavior duo to protein function and activity alteration[104] which can lead to diseases such as neurological disorders[106] .

Due to the presence of a gamma peptide bond between the carboxyl group of glutamate and amino group of cysteine, GSH and GSSG are resistance to the action of cellular

proteases, consequently these are exclusively degraded on the outside of cells that express γ-glutamyltranspeptidase (GGT). GSH and GSSG degradation is a source of amino acids that can be reused for *the novo* synthesis of GSH when necessary[96].

Besides the above-mentioned capabilities of GSH, GSH can also control intracellular redox conditions and protein function through a mechanism call S-glutathionylation, an important mechanism of redox regulation[107].

### 1.6.4 Protein glutathionylation (P-Glu)

Protein S-glutathionylation (P-Glu) is a reversible post-translational modification, which consists in the binding of a GSH or GSSG molecule to thiol group of cysteine residues of proteins forming a mixed disulfide bond between the protein and GSH [108,109]. Cysteine groups within proteins are susceptible to oxidative changes and can act as "redox sensors", in cases of severe stress, these can suffer from irreversible oxidation which can render the protein dysfunctional and let to its destruction. [86].

Not all cysteine residues have the same propensity to be glutathionylated. This propensity depends on (i) the ease of access to the thiol groups in the three-dimensional structure of the protein and (ii) on the reactivity of each cysteine, which depends on pKa, which is affected by neighboring amino acids. These restrictions and conditions contribute to make P-Glu a process with some specificity[108] .

P-Glu can occur spontaneously, stimulated by elevated oxidative and nitrosative stress that greatly rises the levels of GSSG in the cells. Alternatively, and more commonly, it can occur in a regulated manner by the action of enzymes such as glutathione s-transferase or GRX 1 and 2, under controlled and physiologic contexts like cell differentiation, cell growth and physiologic fluctuated ROS levels, which contributes to its view as an adaptative mechanism [100,108]. Additionally, P-Glu is also a way to keep the cellular levels of GSSG low and store glutathione inside the cells [104].

S-Glutathionylation can act as a protective mechanism against oxidative stress, as it prevents the irreversible oxidation of thiol groups from cysteine residues of proteins and consequent alteration or loss of protein function [104] . It can also be a regulatory mechanism of protein function, since the formation of disulfides alters the conformation and aggregation of proteins

and modulates protein activation or inhibition. Thus P-Glu is capable of influencing signal transduction[109,110].

Accumulating evidence suggests that GSH and P-Glu reactions have a central role in controlling several cellular processes in response to changes in the redox environment. Glutathionylation occurs in a wide range of target proteins that are essential to cell growth, differentiation, cell metabolism, apoptosis.[111,112] As an example, it has been shown that adenine nucleotide translocase (ANT), a protein that controls ADP/ATP exchange in the IMM, has its pore forming activity controlled by P-Glu. P-Glu of ANT protects critical thiol groups and avoids the nonspecific pore forming activity of ANT which leads to mitochondrial permeabilization and apoptosis induction[113]. Likewise, the glycolytic enzyme, glyceraldehyde-3-phosphate dehydrogenase, which has a primary role in glycolysis and energy production, has been shown to be inactivated by S-glutathionylation[114], which favors the channeling of glucose to the pentose phosphate pathway and provides NADPH (reductive power) for antioxidant defenses at the expense of glycolysis, this reduces the ROS production by electron transport chain and promotes the reestablishment of the redox buffering power of the cells [112]. Other targets include Nf-Kb and p53 [115].

Being P-Glu a reversible regulatory mechanism, when normal levels of oxidant species are again reached, and the reducing cellular environment is regained with GSH/GSSH in normal levels, protein deglutathionylation occurs spontaneously or is mediated by GRX 1ou 2 allowing the establishment of basal protein state [86] .

## 1.7 Objectives

Mitochondria are key regulators of cell fate, in fact, damaged mitochondria are like ticking time bombs that detonate if the clock is not stopped, thus they must be rapidly eliminated to avoid cell damage and death. Mitophagy is the process by which cells are able to eliminate damaged or excessive mitochondria, their removal is essential to prevent cellular dysfunction. Consequently, mitophagy can be considered a cytoprotective mechanism. In stroke and other pathological conditions characterized by oxidative stress and dysfunctional mitochondria, mitophagy can a be a valuable process to limit cell damage and/or cell death. Here, we aim to

deeply explore redox molecular pathways underlying mitophagy for its potential use as cyto-protective process.

In the literature, it has been demonstrated that both CCCP (a mitochondrial uncoupler) or/and ROS trigger mitophagy through PINK1/PARKIN pathway by inducing mitochondrial recruitment of PARKIN and stabilization of PINK1 in the OMM[75,116,117]. Our premise is that in response to mild stress, mitochondria produce signaling levels of ROS that in turn induce mitophagy for the elimination of dysfunctional mitochondria, being a cytoprotective cellular process [43] .

We hypothesized that mitophagy induction can be regulated by GSH signaling, namely that the accumulation of mitochondrial ROS stimulates the production and oxidation of GSH, which would stimulate mitophagy *via* protein S-glutathionylation of key mitophagy related proteins. In fact, unpublished and preliminary data from our lab show that CCCP-induced mitophagy is associated with glutathionylation of PINK1 and PARKIN in primary culture of astrocytes and purified mitochondria from adult mouse brain cortex (Figure A.1).

In order to test our hypothesis, several specific aims were followed using SH-SY5Y neuroblastoma cell line and the transgenic cell line SH-SY5Y mitoQC (mitophagy reporter):

1) To confirm that CCCP can trigger mitophagy, but not cell death and optimize new read outs for mitoQC reporter.

2) To explore whether ROS-induce mitophagy depends on GSH levels and GSH signaling, namely by assessing protein S-glutathionylation of mitophagy-related proteins.

3) To confirm that GSH signaling has a role in mitophagy process by limiting GSH levels. For that the expression levels of the rate limiting enzyme for GSH production, GCLC, will be knock down and mitophagy will be measured.

The final aim is to explore a potential novel molecular mechanism underlying mitophagy activation given the importance of mitochondria in oxidative stress related injuries and potential as therapeutical target. Protecting cells (e.g. neurons and glia) from cell death by targeting mitochondrial quality control, in particular by boosting mitophagy to reduce oxidative stress and avoid cell death is a possible way to contribute to better outcomes in neuronal diseases such as stoke.

# 2

# MATERIALS AND METHODS

## 2.1 Main used buffers

The composition of the main used buffers for cell culture and western blot techniques are described in Table 2.1 . Working solutions correspond to once concentrated buffer solutions, unless stated otherwise in the respective section.

Table 2.1 **Buffers composition**

| | |
|---|---|
| PBS 10x | 1,54 M NaCl, 15,4 mM $KH_2PO_4$, 34 mM $Na_2HPO_4$; pH =7.2 |
| RIPA 10x | 50 mM Tris-HCl,150 mM NaCl, 3.4mM SDS, 24mM sodium deoxycholate, 40mM Triton X-100, 1% proteases inhibitors (Invitrogen) |
| LB 5x | 1.5mM Tris-HCl, 10% (w/v) SDS, 25 mL glycerol (Sigma), 2.5 mL β-mercaptoethanol (Sigma), 2.5mL bromophenol blue (Sigma); pH=6.8 |
| T-TBS 10x | 3M NaCl, 1M Tris-HCl |
| 5% (w/v) BSA | 5g BSA (EMD Millipore), 100ml T-TBS 1x |

## 2.2 Cell culture model for mitophagy assessment

In this work, human neuroblastoma SH-SY5Y cell line and transgenic SH-SY5Y mitoQC cell line were used. SH-SY5Y mitoQC cells express mitochondrial fission 1 (FIS1) protein with a fused mCherry-green fluorescent protein (GFP) tag (Figure 2.1). GFP is excited at maximum near 488nm and emits near 509nm, while mCherry is excited at maximum at 561nm, emitting maximum near 610nm. MitoQC reporter is based on the different acid-labile properties of these proteins. Whenever mitophagy occurs, mitochondria enter into lysosomes and GFP fluorescence is quenched due to the low pH, while mCherry's is intact, so only red fluorescence

is present (Figure 2.1) [118]. Thus, mitophagy can be quantified by assessing the number of red-only puncta present, which represents mitolysosomes.

SH-SY5Y mitoQC cell line was the prevalent model used in this study, with SH-SY5Y cells being used when fluorescence assays not related to mitophagy were necessary.

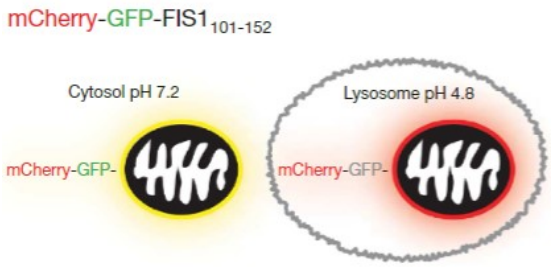


Figure 2.1 **Schematic representation of mitoQC reporter principle**. In steady state both GFP and mCherry fluoresce, green and red, respectively, which merges into a yellowish color signal. When mitochondria endure mitophagy, GFP fluorescence is quenched due to the lower pH, and only mCherry (red) fluorescence is present in the mitolysosomes. Adapted from [130]

## 2.3 Cell culture maintenance

SH-SY5Y and the transgenic mitoQC SH-SY5Y cell lines were maintained at 37ºC, in an incubator with 5% $CO^2$ atmosphere in growth medium DMEM-F12 (Dulbecco's Modified Eagle Medium: Nutrient Mixture F-12) (Gibco and Biowest) enriched with 10% Fetal Bovine Serum (FBS; inactivated, Gibco), 2% Penicillin+Streptomycin (P/S; Gibco) and, in the case of mitoQC cells, 1% Hygromycin B (Invitrogen).

Cells were grown in 75$cm^2$ t-flasks (Falcon®) and subcultured twice a week with a dilution of 1/3 or 1/4 in order to provide fresh nutrients and growing space to ensure continually growing cells.

Since these are adherent cells, they were enzymatically separated and detached from the plastic. Accordingly, the growth media was discarded, cells were washed with 5ml phosphate buffered saline (PBS; Table 1) before adding 3ml of Trypsin /EDTA (Gibco™) for 3min at 37ºC. Next, 3 mL of fresh culture medium was added to inhibit Trypsin's action and cell suspension was homogenized. The cell suspension was then plated into the different plates depending on the used technique, or into a new 75$cm^2$ t-flash for cell culture maintenance.

## 2.4 Cell thawing and freezing

For cell thawing, frozen cells were rapidly thawed by hand, transferred into a 15ml falcon tube (VWR) with 4ml of DMEM F12 supplemented with 10 % FBS and 2 % P/S and centrifuged at 500g for 5min. The supernatant was discarded, and cell pellet resuspended with 5ml of growth medium. After homogenization, cell suspension was transferred to a 75cm$^2$ t-flask and a further 5ml of growth medium were added. Cells were let to grow until confluence was reached.

For cell freezing, after detachment of the cells via trypsinization, cell suspension was centrifuge in a 15ml falcon for 5min at 500g, the supernatant was discarded, and the pellet resuspended with 1ml of freezing solution (90% FBS and 10% dimethyl sulfoxide (DMSO; sigma)). The suspension was transferred to a cryotube (Thermoscientific), wrap with tissue paper and placed in a styrofoam holder at -80°C.

## 2.5 Western blot

### 2.5.1 Sample preparation

The western blot technique was used to semi-quantify protein levels between differently treated samples. SH-SY5Y mitoQC cells were seeded at 50% confluence (1,25*10$^5$ cells/well) in 6 well plates (Falcon) and treated with carbonyl cyanide m-chlorophenylhydrazone (CCCP; final concentration of 25 μM) for 1h. The supernatant was discarded, and the cells washed twice with PBS. Then, 300 μl of radioimmunoprecipitation assay buffer (RIPA, Table 2.1) were added for cell lysis, followed by up and down movement with the micropipette for mechanical shearing of the cell membrane. The cell lysates were then recovered and frozen at -20ºC.

### 2.5.2 Immunoblotting

The samples were denatured with loading buffer 5x (LB; Table 2.1) for 5 min at 95ºC. These were loaded into 1mm thick 10% or 12% polyacrylamide gels (Table 2.2) and separated by electrophoresis under reducing conditions. To monitor protein separation, 4 μl of NZYColour Protein Marker II (NZYTech) were also loaded. After electrophoresis running with the conditions varying between 1h30min-2h at 150-200mv, proteins were electrically transferred from

the gel to nitrocellulose membrane (Amersham ™) for 1h30min at 0,5A. Next, membranes were stained with Ponceau Red (Biotium) for successful protein transfer verification and protein load quantification whenever necessary. The excess Ponceau Red was removed with milliQ $H_2O$, and the membranes were scanned inside a plastic pocket for further protein quantification purposes.

Table 2.2 **Polyacrylamide gels composition**

| | |
|---|---|
| Separating gel buffer (pH = 6.8) | 0.5M Tris-HCl (OmniPur), 13.8mM SDS, 1L milliQ H2O |
| 12% polyacrylamide separating gel | 1.7 ml milliQ H2O, 2 ml 30% acrylamide/Bis (BioRad, # 1610156), 1.25 ml separating gel buffer, 50 µL APS 10 % (Sigma),5 µL TEMED (Sigma) |
| 10% polyacrylamide separating gel | 2.05 ml milliQ H2O, 1.65 ml 30% acrylamide/Bis, 1,25 ml separating gel buffer, 50 µL APS 10 % ,5 µL TEMED |
| Stacking Buffer (pH= 8.8) | 1.5M Tris-HCl, 13.8mM SDS, 1L milliQ H2O |
| Stacking gel | 1.5 mL milliQ H2O, 0.325 mL 30% acrylamide/Bis, 0.625 mL Stacking Buffer, 25 µL APS 10 %, 5 µL TEMED |

Then, the membranes were blocked with a 5% (w/v) bovine serum albumin (BSA) solution diluted in Tween-Tris-buffered saline 1x (T-TBS; Table 2.1) for 1 hour under agitation at room temperature (RT) or overnight at 4ºC. Next, the membranes were incubated for 2 hours under agitation at RT or overnight at 4ºC with primary antibodies against PINK1 (1:1000 in 5% BSA solution; Cell Signaling #6946), GCLC (1:1000 in BSA 5% solution; AA 528-637) or Actin (1:5000 in BSA 5% solution; Sigma A5441). Blots were developed using an enhanced chemiluminescence detection kit (Clarity™, Biorad) after incubation with horseradish peroxidase-conjugated secondary antibodies anti-mouse IgG (1:5000 in BSA 5%; NA931V) or anti-rabbit (1:5000 in BSA 5%; NA934v, Amersham ™) for 1 hour at RT under agitation. Membranes were developed with X-ray films (Amersham ™) and reveled in the absence of light using developer (Carestream, 5158621) and fixating solution (Carestream, 5158639). Dried X-ray films were then digitalized or photograph over a light box, and protein quantification was done using Image J software. For loading control and protein normalization, actin or Ponceau red stained membrane scans were used for total cellular extract, for mitochondrial fractions succinate dehydrogenase

complex, subunit A (Western blot Cocktail, MitoSciences, MS1032) or Ponceau red stained membrane scans were used.

## 2.6 Protein quantification

For protein quantification, Pierce™ BCA Protein Assay Kit (ThermoScientific™) was used. Samples were diluted into milliQ $H_2O$ 1:10 and plated on a 96-well clear plate (SARSTEDT). Then, 100 µl of bicinchoninic acid (BCA) working reagent (50:1, Reagent A:B from kit) were added to each well and incubated at 37°C for 30 min. Afterwards, absorbance at 465nm was measured using TECAN infinite F200 PRO spectrofluorometer. A standard curve based on different known concentrations of BSA (from 1000 µg/mL to 7,812 µg/mL) was calculated by linear regression for sample protein quantification.

## 2.7 Mitochondrial fraction preparation

SH-SY5Y mitoQC cells were grown in 175cm2 t-flasks until 100% confluence, then cells were treated with CCCP at final concentration of 25 µM for 1h. Afterwards, cells were washed with ice-cold PBS and recovered after detached by trypsinization. The cellular suspension was centrifuged for 5 min at 500g, the supernatant was discarded, and the cells were washed with PBS by centrifugation for 5min at 500g. The supernatant was discarded, and the pellet was homogenized and incubated in 3,5mL of hypotonic buffer (0.15mM $MgCl_2$, 10mM KCl, 10mM Tris-HCL, pH 7.6) for 5min at 4°C for mild swelling. Then, 3,5mL of twice concentrated homogenization buffer (0.15mM $MgCl_2$, 10mM KCl, 10mM Tris-HCL, 0.4mM phenylmethylsulfonyl fluoride, 250mM saccharose, pH=7.6) were added into the samples for reaching normal osmolarity. Then cells were manually lysed using a Douncer homogenizer (Wheaton) by doing fifty up and down movements with each pestle. Cellular suspension was centrifugated for 10min at 900g for the elimination of entire cells and nuclei. Then sample supernatant was centrifuged for 10min at 10000g (4ºC) for mitochondrial enriched fraction precipitation. The mitochondrial pellet was recovered and resuspended in 130 µl of homogenization buffer 1x (1 ml of homogenization buffer 2x + 1ml of milliQ $H_2O$). Total protein amount in the mitochondrial fraction

samples was quantified by Pierce™ BCA assay. All the procedure was performed in ice to avoid protease activity and protein degradation.

## 2.8 Immunoprecipitation of proteins in mitochondrial fraction

SH-SY5Y mitoQC cells were grown in 175cm2 t-flasks almost until confluence and treated with 25 µM CCCP for 1h. The protocol described in the section above was followed to recover mitochondrial enriched fractions. From these samples, 100 µg of protein were retrieved and diluted into 100 µl of homogenization buffer 1x with 0.5% of Triton X-100 for mild permeabilization of outer mitochondrial membrane. Next, samples were incubated with 20 µL of anti-GSH antibody (1mg/ml; 101-A Virogen) for 1h30min at 37°C under mild agitation. Then 15 µL of protein A/G agarose beads (Santa Cruz Biotechnology, sc-2003) were added for 30min at 37°C in order to precipitate anti-body-protein complex samples. Samples were centrifuged for 10min at 10000g, the supernatant was discarded, and the beads were wash three time with PBS at 1000g. Finally, samples were detached from the beads using 40 µL of LB, and then frozen at -20°C for later immunodetection *via* western blot.

## 2.9 ROS generation measurement

ROS generation was followed by $H_2$DCFDA/DCF assay. In this assay, the amount of $H_2O_2$ generated by the cells was assessed by the conversion of 2',7'-dichlorofluorescein diacetate ($H_2$DCFDA) (Invitrogen) into fluorescent 2',7'-dichlorofluorescein (DCF).

SH-SY5Y cells were plated at $4.25*10^3$ cells/well in clear bottom black 96 well plates (BrandTech®, 781971). Forty-eight hours later, cells were treated with 25µM CCCP for 1hour, the supernatants were discarded, the cells were washed twice with PBS and incubated for 20 min at 37°C with PBS containing 5µM of $H_2$DCFDA. After the incubation, fluorescence levels were measured at $\lambda_{ex}$ 485 nm/$\lambda_{em}$ 535 nm using a microplate reader (TECAN infinite F200 PRO spectrofluorometer).

## 2.10 Mitophagy assessment using mitoQC model

For mitophagy assessment based on mitoQC reporter, three different and complementary approaches were conducted:

### 2.10.1 Fluorescence microscopy assessment of red-only puncta (mitolysosomes)

SH-SY5Y mitoQC cells were seeded at 40% confluence ($2*10^4$ cells/well) on glass coverslips (VWR) in 24 well plates. After 20h, cells were treated with CCCP for 1h at 25 µM. After treatment, cells were washed twice with PBS, fixed with 4% of paraformaldehyde (PFA) (3,7 % (w/v) PFA, 200mM HEPES (Sigma); pH=7) for 15 min and then washed again twice with PBS. Then the coverslips were mounted onto glass slides with Prolong mounting medium (Invitrogen).

Images were taken using confocal Zeiss LSM980 and for their analysis ImageJ software was used. Using a *MitoQC* plugin kindly provided by Beatriz Villarejo Zori, PhD (Biological Research Center Margarita Salas, Madrid, Spain), the quantification of green and red fluorescence intensity was done. Green and red fluorescence values were scatter into a plot and a threshold of elevated red fluorescence (>75%) and low green fluorescence (<25%) was set to define mitolysosomes. The number of mitolysosomes (red-only puncta) was obtained and normalize by the number of nuclei to assess mitophagy for each condition. The number of nuclei were manually counted using cell counter plugin.

### 2.10.2 SH-SY5Y MitoQC fluorescence quantification on the microplate reader

SH-SY5Y mitoQC cells were seeded in clear bottoms black 96-well plates (Nunc and Brand 78171) at 70% confluence ($6*10^3$ cell/well) and, on the next day, treated with CCCP for 1h. Green fluorescence was measured 485 $\lambda_{ex}$/ 535 $\lambda_{em}$ nm and red fluorescence at $\lambda_{ex}$ 560nm /$\lambda_{em}$ 635 with TECAN infinite F200 PRO spectrofluorometer. In order to access mitophagy, the ratio of red (mitolysossomes and cytosolic mitochondria) to green (cytosolic mitochondria) fluorescence was calculated and compared between the different conditions.

## 2.10.3 Flow Cytometry measurement of mitoQC reporter

SH-SY5Y mitoQC cells were plated at 40% confluence in 24 well plates ($2*10^5$ cells/well). Two days later, cells were treated with 25 μM CCCP for 24h and 1h. After treatment, the supernatant was recovered, cells were washed with 100 μl PBS, trypsinized (150μl) for 3 min at 37 ºC and resuspended in medium for Trypsin inactivation. Using Attune® Acoustic Focusing Cytometer (Thermo Scientific), 10000 cells were acquired for analysis. To excite the cells a blue laser (488nm) was used, green (GFP) and red (mCherry) fluorescence emissions were detected at 530nm±15nm and >640nm, respectively. The gating strategy followed is displayed in Figure 2.2 . When mitochondria of mitoQC cells undergo mitophagy, the fluorescence of GFP (green) is lost due to the low pH of mitolysosomes while mCherry's (red) remains intact. Accordingly, cells with high mitophagy rates should present high red and low green fluorescence emission. Thus, a conceptual gate representative of cells with high emission in BL3-A (640nm;red) and low at BL1-A(530nm;green) was designed ( "mitophagy+").

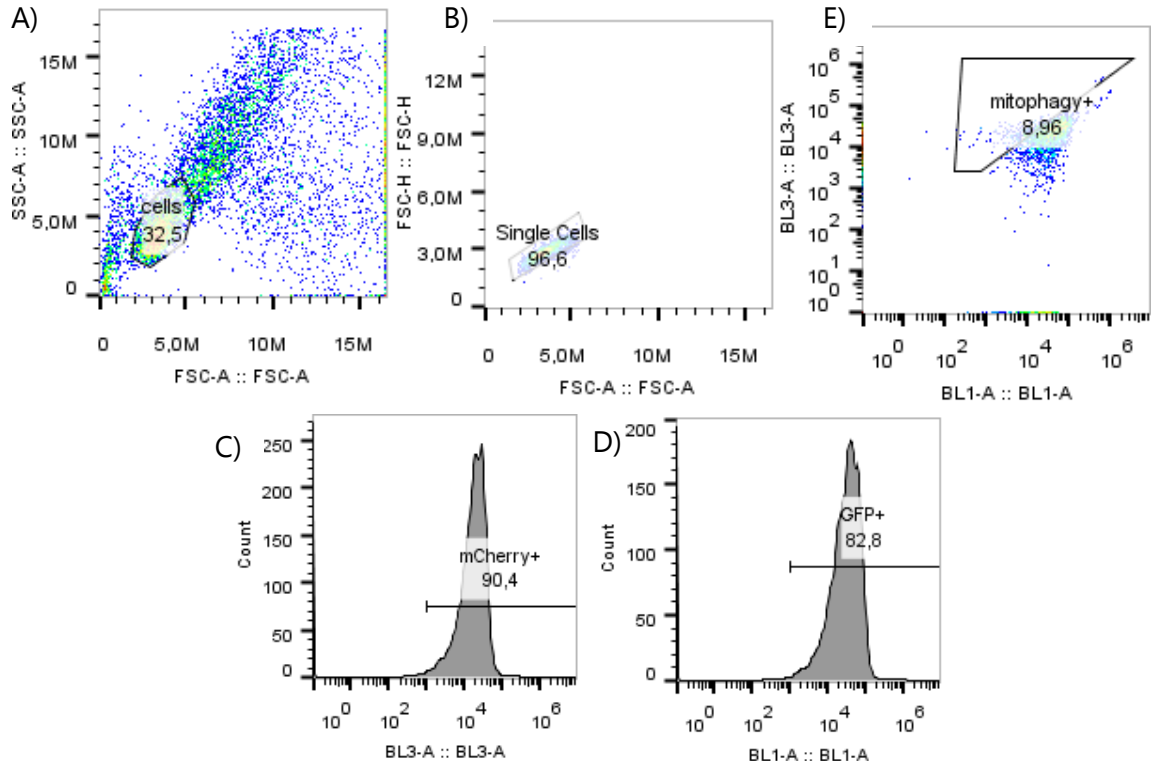


Figure 2.2 **Flow cytometry gating strategy** A) SSC vs FSC density plot. Each dot represents an individual event, a gate was applied to avoid debris and dead cells and select a specific population. B) FCS height vs FCS area plot. A gate was applied to exclude doublets and select single cells C) Single- parameter histogram to evaluate relative mCherry expression, positive dataset considered when light scatter intensity)> $10^3$ D) Single- parameter histogram to evaluate relative GFP expression, positive dataset considered when light scatter intensity)> $10^3$ E) mCherry vs GFP density plot. a gate was applied to select cells undergoing high mitophagy rates (elevated emission at BL3-A (640nm;red) low at BL1-A(530nm;green)

## 2.11 siRNA GCLC transfection

SH-SY5Y mitoQC cells were transfected with small interfering RNA (siRNA) coding for glutamate cysteine ligase- catalytic subunit (GCLC) (Ambion #144714) using Lipofectamine ™ RNAi MAX (Invitrogen) and Opti-MEM medium (Gibco) to silence GCLC expression. Firstly, an optimization for the amount of siRNA to used was done. Cells were plated in 24w and 12w plates at 40% confluence, and transfected for 24h or 48h with 5, 10 or 15 pmol of siGCLC per well. For each plate, solutions A and B for every siRNA GCLC concentrations were prepared according to Table 2.3 and Table 2.4 , then each solution B was added to the respective solution A and gently mixed for 20 min to form liposomes at room temperature. Then, cells were transfected with the respective solutions and growth medium without antibiotics was added (200 µL for 24W and 400 µL for 12w plates). Four hours after transfection, growth medium with twice antibiotics was added (250 µL for 24W plates and 500 µL for 12w plates). After 24h or 48h samples were recovered. GCLC expression was assessed by Western blot assay (Figure 2.3).

Table 2.3 **24 well plate siRNA GCLC optimization solutions**

| siGCLC concentration per well | Solution A per well | Solution B per well |
|---|---|---|
| 0 pmol siRNA | 25 µL of Opti-MEM® | 25 µL of Opti-MEM® |
| 5 pmol siRNA | 0,5 siRNA GCLC<br>25 µL of Opti-MEM® | 25 µL of Opti-MEM®<br>0,5 µL of Lipofectamine™ |
| 10 pmol siRNA | 1 µL siRNA GCLC<br>25 µL of Opti-MEM® | 25 µL of Opti-MEM®<br>0,5 µL of Lipofectamine™ |
| 15 pmol siRNA | 1,5 µL siRNA GCLC<br>25 µL of Opti-MEM® | 25 µL of Opti-MEM®<br>0,5 µL of Lipofectamine™ |

Table 2.4 **12 well plate siRNA GCLC optimization solutions**

| siGCLC concentration per well | Solution A per well | Solution B per well |
|---|---|---|
| 0 pmol siRNA | 50 µL of Opti-MEM® | 50 µL of Opti-MEM® |
| 5 pmol siRNA | 1 µL siRNA GCLC<br>50 µL of Opti-MEM® | 50 µL of Opti-MEM®<br>2 µL of Lipofectamine™ |
| 10 pmol siRNA | 2 µL siRNA GCLC<br>50 µL of Opti-MEM® | 50 µL of Opti-MEM®<br>2 µL of Lipofectamine™ |
| 15 pmol siRNA | 3 µL siRNA GCLC<br>50 µL of Opti-MEM® | 50 µL of Opti-MEM®<br>2 µL of Lipofectamine™ |

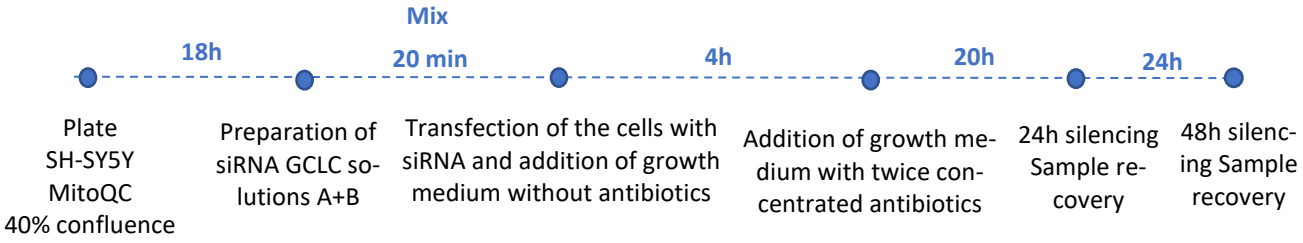


Figure 2.3 **Schematic representation of siRNA GCLC transfection protocol**

## 2.12 Glutathione Quantification

### 2.12.1 Sample preparation

For glutathione levels quantification, SH-SY5Y mitoQC cells were seeded at 40% confluence (2*$10^4$cells/well) in 24 well plates (Falcon) and treated with: 25 µM CCCP for 1h or 10 µM CCCP for 24h (Figure 2.4).

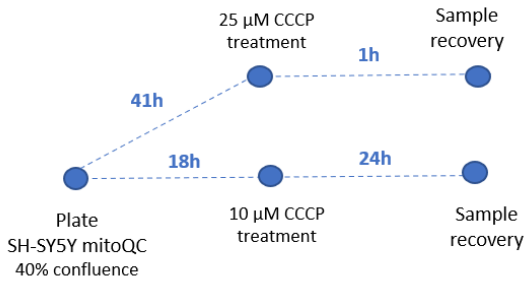


Figure 2.4 **Basic sample preparation protocol for GSH quantification**

Additionally, SH-SY5Y mitoQC cells were seeded at 40% confluence in 24 well plates and GCLC expression was silenced using 15pmol *per* well of siRNA GCLC for 48h. After 24h of transfection, cells were treated with 10 µM CCCP for 24h. One hour before completing 48h of transfection, the remaining cells were treated with 25 µM CCCP for 1h (Figure 2.5). Then, cells supernatants were removed, and each well was washed twice with PBS. Next, 200 µl of 5-Sulfosalicylic Acid 5% (w/v) (Sigma, S 2130) were added to each well and cells scraped and recovered using a micropipette. Following, two cycles of freezing and thawing were done using liquid nitrogen (10seg) and water bath at 37°C (1min30sec) for cell lysis. Next, samples were kept at 4°C for 5 min and then centrifuged at 10000g for 10min. The supernatants containing GSH were recovered and kept at -20°C for further quantification.

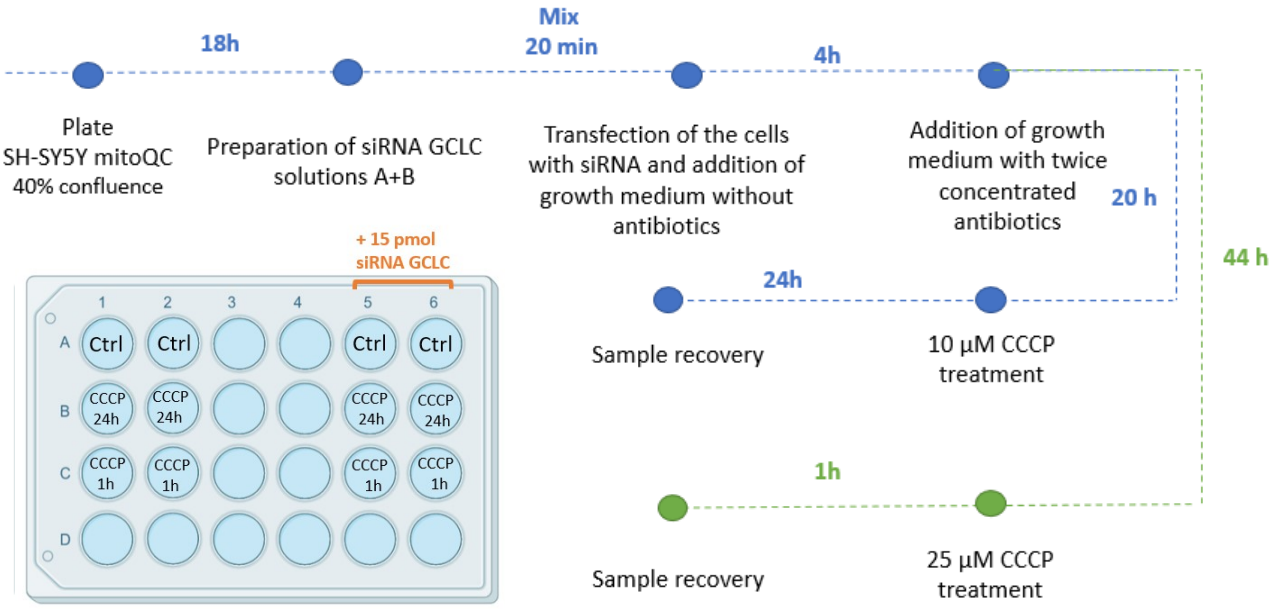


Figure 2.5 **Schematic representation of experimental protocol and plate design followed for the preparation of samples with silenced GCLC with the intent of GSH quantification.**

## 2.12.2 GSH and GSSG quantification

This glutathione quantification method is based on (i) the reaction between GSH and 5,5'-dithio-bis-(2-nitrobenzoic acid) (DTNB) and (ii) the recycling of GSSG by GR (Figure 2.6).

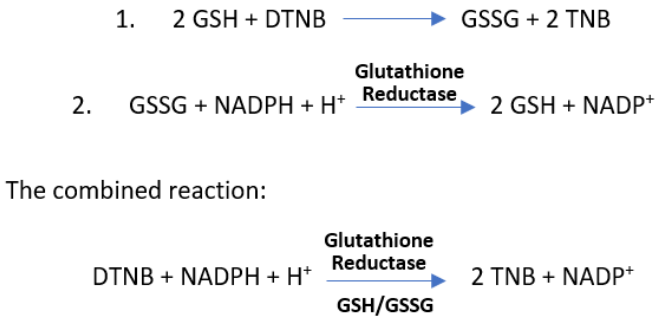


Figure 2.6 **GSH and GSSG quantification reaction equations**

First, GSH present in the samples reacts with DTNB, which generates oxidized GSSG and 5-thio-2-nitrobenzoic acid (TNB), a yellow-colored compound whose absorbance can be measured. Then, in order to quantify the total amount of glutathione present in the samples, GSSG is reduced into GSH by GR in the presence of NADPH, which provides reductive power. Thus, GSH is continuously generated and continuously reacts with DTNB, so the concentration of

TNB is directly proportional to total amount of reduced GSH and oxidized GSSG present in the samples.

Samples were thawed and 34.5 µL of each sample were added into a transparent 96 well plate. A working solution (Table 2.5) was prepared and add to each well. The plate was shaken for 1 min and incubated for 3 min at 30°C in TECAN infinite F200 PRO spectrofluorometer. Next, 20µl of 50µM glutathione reductase (Sigma #G3664) were added to each well, the plate was shaken for 30 seconds and the absorbance at 415nm was read for 5min with 45sec intervals. A GSH calibration curve was also done with standard GSH (Sigma #G 4251) prepared in assay buffer with concentrations ranging from 0 µM to 0.513 µM. GSH calibration curve was calculated by linear regression for sample GSH quantification.

Table 2.5 **GSH and GSSG quantification reagents**

| | |
|---|---|
| Stock solution A | 0.12M KH2PO4, 1.19M EDTA, 500ml milliQH2O |
| Stock Solution B | 0.12 M K2HPO4, 1.19mM EDTA, 500ml milliQH2O |
| Assay buffer | to 10 mL of stock solution A add stock solution B until pH=7.0 is reached |
| Working solution per well | 3.7 µL of 3.79mM of DTNB, 9.1 µL of 4.8mM NADPH and 142 µL of assay buffer |

## 2.13 Statistical analysis

Statistical analysis was performed using GraphPad Prism 6 software. Normality was tested using D'Agostino & Pearson omnibus normality test. Statistical comparisons between distinct groups of conditions were analyzed using unpaired student t-test when data were normally distributed or by Mann-Whitney test when data were not normally distributed. P-values lower than 0.05 were considered statistically significant. When possible, the data represent the mean ± standard deviation (SD).

# 3

# RESULTS

## 3.1 ROS generation induced by CCCP

To explore the molecular mechanisms underlying mitophagy, in particular the role of ROS and/or GSH signaling in the progression of this process, the mitochondrial uncoupler CCCP was used at low levels to stimulate mitophagy via ROS signaling. In fact, it has been shown that CCCP-induced mild uncoupling generates mitochondrial ROS that are needed for the mitophagic process progression[116,119]. While it is well established that at high concentrations CCCP induces cell death by inducing severe mitochondrial oxidative stress and mitochondrial membrane permeabilization [120].

Thus, the first task required for this work was to verify that CCCP stimulates ROS production in our model, SH-SY5Y cells. For this, and based on previous work in our lab, a 1-hour treatment with 25μM of CCCP was chosen, since under these conditions there is no cell death. The cell-permeable probe $H_2$DCFDA was chosen for the quantification of $H_2O_2$ levels, the most stable and important signaling ROS in the cells. In this assay, $H_2$DCFDA is oxidized to the fluorescent DCF by $H_2O_2$, thus DCF fluorescence levels are directly proportional to $H_2O_2$ levels.

The results (Figure 3.1) show an increase in ROS ($H_2O_2$) generation in CCCP treated cells of about 40% compared to control. These results were expected and are in agreement with what is stated in the literature [76] , as well as with previous results generated in our lab using mice primary culture of astrocytes (Figure A.2). In conclusion, as expected CCCP increases ROS generation using SH-SY5Y cell line.

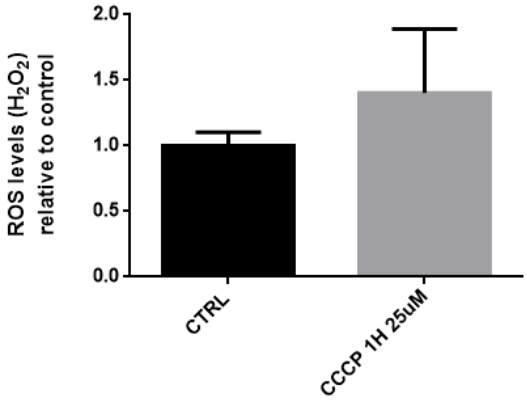


Figure 3.1 **Determination of cellular ROS ($H_2O_2$) levels by $H_2$DCFDA/DCF assay**. SH-SY5Y cells were treated with 25μM CCCP for 1h. Values were normalized over control. Graphs represent the median ± SD of three (control) and four (CCCP) technical replicates of one biological experiment. This experiment was performed three times with similar results.

## 3.2 CCCP and mitophagy

In order to analyze whether mitophagy mechanisms depend on ROS signaling, SH-SY5Y mitoQC cell line was used, as it allows to assess in an accurate manner the mitophagic process. Thus, CCCP ability to induce mitophagy in our hands was confirmed using the mitoQC reporter. Likewise, we also took the opportunity to test new techniques and possible readouts to measure mitophagy using the mitoQC reporter present in this cell model. Usually, mitoQC reporter quantification of mitophagy is done by fluorescent confocal microscopy. However, this technique is time consuming and semi-quantitative since it is based on imaging analysis. Thus, quicker and easier approaches are needed.

### 3.2.1 Assessing mitophagy with confocal microscopy

Confocal microscopy is a classical widely used technique for quantify mitophagy using fluorescent probes. By evaluating proteins co-localization and differences in fluorescence intensity between different conditions, mitophagy can be assessed. Therefore, we used this technique to evaluate whether under our conditions CCCP induces mitophagy using mitoQC reporter.

Considering that co-localized green and red dots represent cytosolic mitochondria and that red-only dots represent mitolysosomes, by the quantification of red-only dots we are able to analyze mitophagy rates differences between the different conditions. SH-SY5Y mitoQC cells were treated with 25 μM of CCCP for 1 hour.

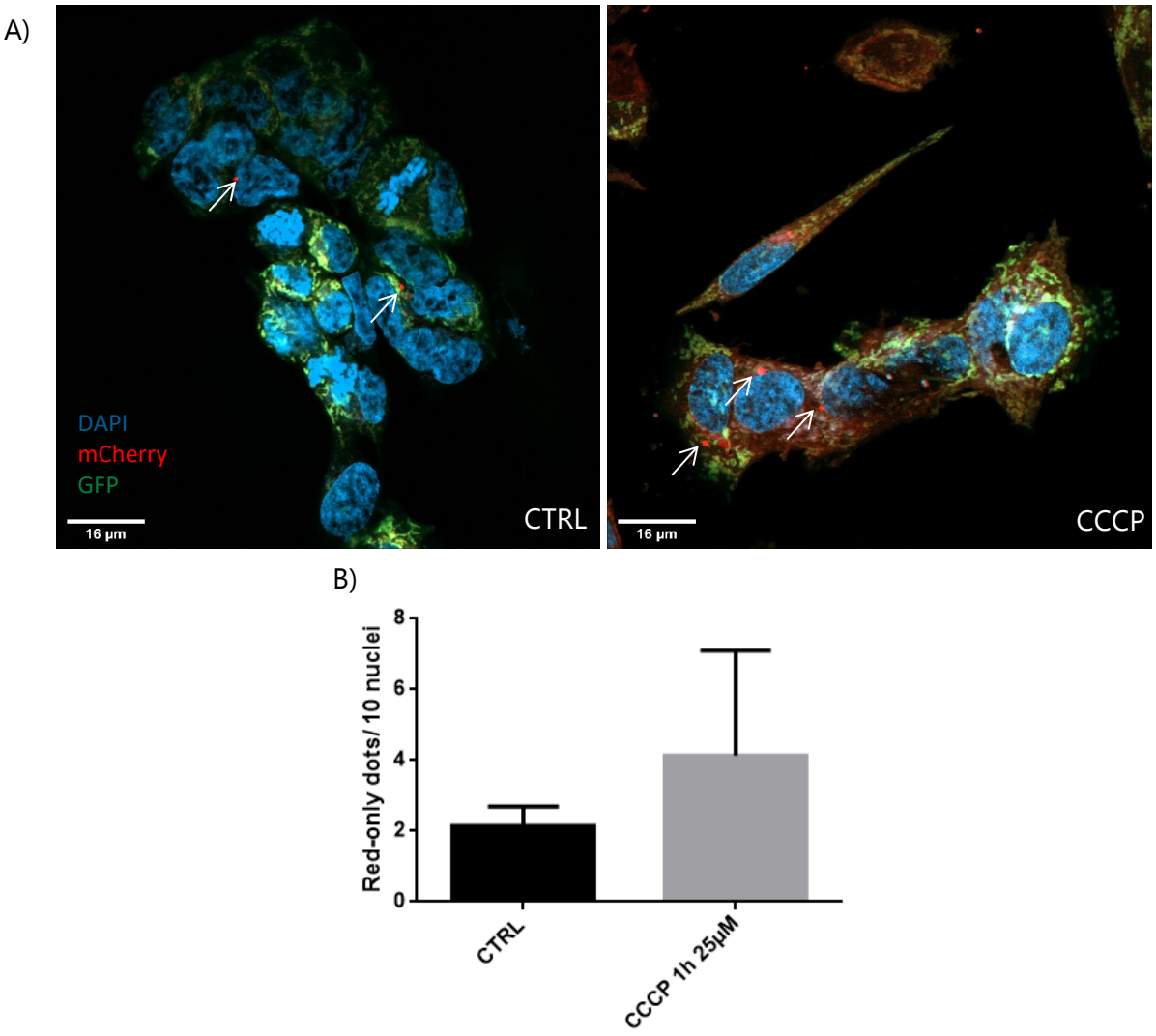


Figure 3.2 **Confocal microscopy images of SH-SY5Y mitoQC cells**. A) Representative Control and 1h 25μM CCCP treated cells confocal images. Red fluorescence represents mCherry and green fluorescence represents GFP. Red-only dots represent mitolysosomes (exemplified by the white arrows). Nuclei were stained using DAPI (Blue). Magnification 630x. Scale bar 16μm. B) Graph representing the number of red-only dots (mitolysosomes) per 10 nuclei of SH-SY5Y mitoQC cells. The results represent the average± SD of three technical replicates from one biological replicate.

These preliminary results (Figure 3.2) show that there is an increase in the number of red-only puncta (mitolysosomes) when mitoQC cells are treated with CCCP, which indicates that the uncoupler is inducing mitophagy. Unfortunately, due to technical problems during co-verslip mounting and image acquisition, this experiment was performed only once.

Nonetheless, this assay is a work in progress, more biological replicates must be done, and optimization of the process achieved. Importantly, these results are in agreement with the literature.

### 3.2.2 Mitophagy quantification based on direct fluorescence measurement using a microplate reader

In order to develop an easier and faster technique to measure mitophagy, we tested for the first time to our knowledge, direct measurement of mitoQC fluorescence using a microplate reader.

To calculate mitophagy rates, red (mCherry) and green (GFP) fluorescence were measured, were red/green fluorescence ratio corresponds to the mitophagy rate. Cells undergoing higher mitophagy rates present an increased ratio of red/green fluorescence.

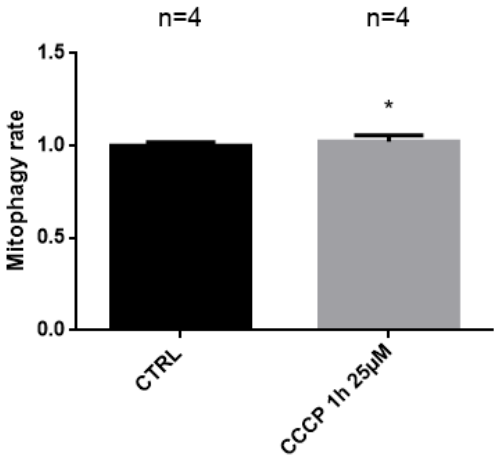


Figure 3.3 **Mitophagy rates in non-treated and CCCP treated cells measured in a microplate reader**. Cells were non-treated or treated with 25µM CCCP for 1h. Green fluorescence values were obtained at 485 $\lambda_{ex}$/ 535 $\lambda_{em}$ nm and red fluorescence at $\lambda_{ex}$ 560nm /$\lambda_{em}$ 635, and ratio GFP/mCherry fluorescence calculated. Ratio values were normalized over control average rate. Graphs represent average ± SD of four biological replicates with a total 21 technical replicates. Differences between experimental conditions were analyzed by unpaired student t-test. The results were considered statistically different when p-value < 0.05.(confidence level of 95%). *p<0.05

Although the differences are very small, the results (Figure 3.3) show that CCCP treated cells have a significant higher mitophagy rate than control cells, which is in line with the expectations, since CCCP is the most classic chemical inducer of mitophagy [76,121].

Nonetheless, caution must be taken when using this technique since the fluorescence measured by the spectrometer includes the fluorescence of all of the cells within the well. Thus, the fluorescence measured may not exactly represent mCherry-GFP-FIS1 tag present in the

mitochondria, but also autofluorescence and fluorescence emission from death cells. To validate this technique for mitophagy assessment, more tests must be done using positive and negative controls of mitophagy. As well, complementary techniques like fluorescence microscopy, must be performed to confirm the results.

Nevertheless, based on the significant results obtained, direct fluorescence measurement with a microplate reader can be used as an easy quick checker for mitophagy, still other robust tests and techniques must be used in order to confirm the results obtained until further validation of this method.

### 3.2.3 Mitophagy assessment with flow cytometry using mitoQC reporter

Flow cytometry is an easy, fast, quantitative technique that allows the determination of the mitochondrial population by detecting protein fluorescence, in this case fluorescence from GFP-mCherry-FIS1 tag. Flow cytometry has already been used to determine mitophagy using a similar mitophagy reporter, mt-Keima [122] , and indirectly via mitochondrial population quantification using MitoTracker deep red dye [121], a mitochondria-selective probe. Thus, to optimize the use of flow cytometry to detect mitophagy using mitoQC reporter, CCCP-induced mitophagy rates were measured under different conditions (non-treated, 25μM CCCP for 1h or 25 μM for 24h). The gating strategy used to obtain these results is displays in Figure 2.2. Cells under mitophagy correspond to cells in the gate with high emission at BL3-A (640nm;red) but lower emission at BL1-A(530nm;green) (Figure 3.4A)).

The results (Figure 3.4) show that treatment with CCCP for 1h did not induce significant differences in mitophagy rates when compared to control in SH-SY5Y mitoQC cells. On the other hand, treatment with CCCP for 24-hour cells has lower levels of mitophagy, which may be associated with higher rates of cell death, which were reflected by a much greater presence of debris in the SSC-FSC event recorder by the cytometer (Figure A.3). After all, CCCP is a cytotoxic compound that must be used with care to prevent cell death. It seems that the amount of CCCP used defines the boundary between inducing mitophagy or cell death in mitochondria.

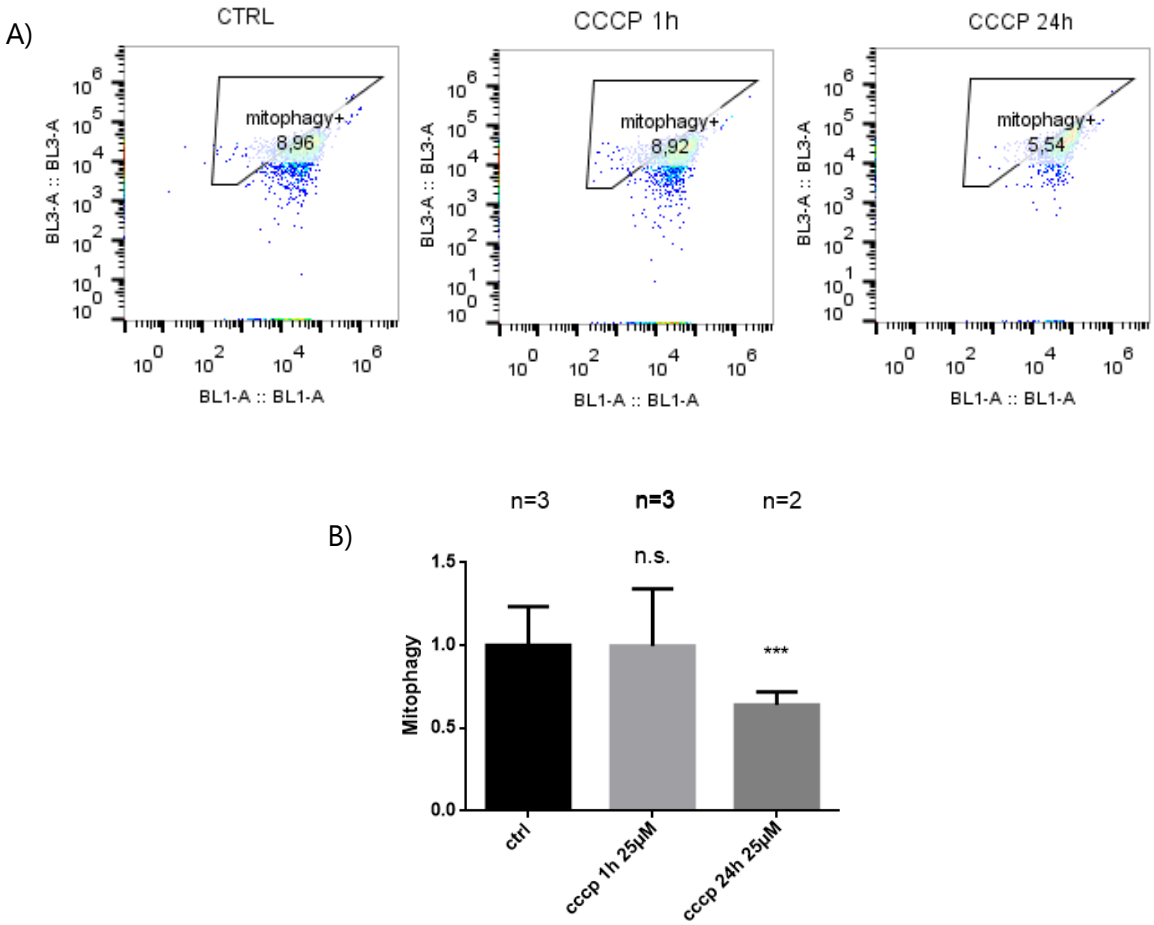


Figure 3.4 **Mitophagy rates in non-treated and CCCP-treated cells obtained via Flow cytometry**. SH-SY5Y mitoQC cells were treated with 25µM CCCP for 1h or 10 µM for 24h, and fluorescence was quantified. Cells were processed, the gating strategy (Figure 2.2) followed, and mitophagy % obtained. A) Representative "mitophagy+" gate profiles for the different conditions (Control; 25 µM CCCP 1h ;25 µM CCCP 24h). These gates represent cells with high mitophagy rates. BL1 detector detects green fluorescence (530 nm+/-15nm) and BL3-A detects red fluorescence (>640nm). B) Mitophagy rates for Control, 25 µM CCCP 1h and 10 µM CCCP 24h conditions. The number of cells in the "mitophagy+" gates for the different conditions were normalized over control average. Graphs represent average ± SD of 2-3 biological replicates with 3 or 5 technical replicates each (13 total for CTRL and CCCP1h;10 total for CCCP24h). Differences between experimental conditions were analyzed by Mann-Whitney test. The results were considered statistically different when p-value < 0.05. n.s.- non-significant; *** p<0.001;

Flow cytometry analysis did not demonstrate that CCCP induces mitophagy, however that does not invalidate CCCP ability to do so, since these experiments were also for technique optimization some considerations must be taken into account. A crucial feature that could have impact the accuracy of the results is that the laser used to stimulate mCherry fluorescence emission had a lower excitation wavelength than the required for maximum signal from mCherry, as well, the emission detector only detected fluorescence with a slightly higher wavelength that the maximum emission pick for mCherry fluorescence. Plus, a third dye to determine cell viability should also be used to warranty mitophagy assessment in live cells only. Moreover, more sample and analysis adjustments (e.g. number of treated cells, passage of the

cells utilized, better definition of the gates) are needed since CCCP is a classical mitophagy inducer, supported on the vast literature demonstrating the ability of CCCP to induce mitophagy [116,121].

## 3.3 PINK1 accumulation in mitochondrial fractions

Previous reports from the literature have shown that CCCP-induced mitophagy occurs in a PINK1/PARKIN dependent manner. In fact, following CCCP treatment and mitochondrial depolarization, PINK1 is stabilized, and PARKIN is recruited on the OMM [70,76,116]. Likewise, assessing PINK1 accumulation in the mitochondria in another strategy to measure mitophagy. Therefore, we tested in our model SY-SY5Y mitoQC cells, whether CCCP is capable of inducing PINK1 stabilization on the OMM. Cells were treated with 25μM CCCP for 1h and mitochondrial fractions were purified for further PINK1 detection by immunoblot. Protein levels of the samples were normalizer using the mitochondrial succinate dehydrogenase complex, subunit A (SDHA) protein.

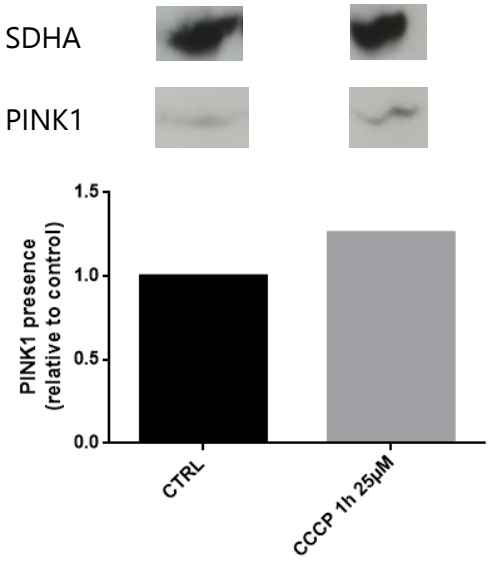


Figure 3.5 **Quantification of PINK1 accumulation on mitochondrial fraction**. Non-treated and treated with 25μM CCCP for 1h SH-SY5Y mitoQC cells. Protein levels were normalized using SDHA mitochondrial protein band intensity. Values presented as relative to control. Graphs represent one biological replicate.

As expected, CCCP treatment induced an increase of about 30% in the accumulation of PINK1 onto the mitochondria (Figure 3.5). Duo to technical problems and delays in the delivery

of PINK1 antibody this experiment was performed only once. Thus, more biological replicates are needed to confirm this find.

Up to this point, all data presented correspond to validation of literature findings, namely confirmation that in our hands and conditions (cell model, concentration, and timing) CCCP promotes mitophagy. In the next subsections data related to GSH signaling are presented.

## 3.4 PINK1 glutathionylation

Our aim focuses on how mitophagy is induced by ROS and GSH signaling. We hypothesize that dysfunctional/depolarized mitochondria produce ROS that can induce mitophagy through GSH signaling, particularly through protein S-glutathionylation (P-Glu). This protein post-translational modification is normally associated with redox changes and is capable of altering protein function and thus of modulating cellular processes such as mitophagy.

Using the human SH-SY5Y mitoQC cell line, we studied mitophagy related proteins, in particular PINK1. PINK1 was chosen because of its key role in CCCP-induced mitophagy. Moreover, it was also targeted because previous results from our lab showing that PINK1 is glutathionylated in mitochondrial fractions purified from primary cultures of astrocytes and adult mice brain cortex following CCCP treatment (Figure A.1). Furthermore, this protein has cysteines residues susceptible to post translational modifications which modulate PINK1 function [123]. Thus, PINK1 is a promising candidate to be regulated by glutathionylation.

To test our hypothesis, we purified mitochondrial fractions of CCCP-treated SH-SY5Y mitoQC cells and immunoprecipitated glutathionylated proteins with an anti-body that recognizes glutathionylated proteins (α- GSH). Then the immunoprecipitated proteins were analyzed by immunodetection using anti-PINK1. Protein quantities were normalize using ponceau staining (Figure 3.6 A))

The results (Figure 3.6) indicate an increase of glutathionylated PINK1 in CCCP-treated condition, suggesting that CCCP in capable of modifying PINK1 by P-Glu. Still, these results come from a single experiment, so further experiments are needed to confirm these results. Likewise, other accurate techniques (such as mass spectrometry) are necessary to confirm that

it is indeed PINK1 that is glutathionylated and not another protein, since protein complexes with glutathionylated proteins must exist and can be co-immunoprecipitated.

Nevertheless, this result is a positive indication that there is a connection between P-Glu and PINK1/PARKIN mitophagy. Suggesting that reversible P-Glu can be an adaptation to redox changes, such as those imposed by CCCP treatment, and act as mediator to adapt ROS production in the mitochondria and promote cell survival, for example through activation of mitophagy via PINK1 glutathionylation.

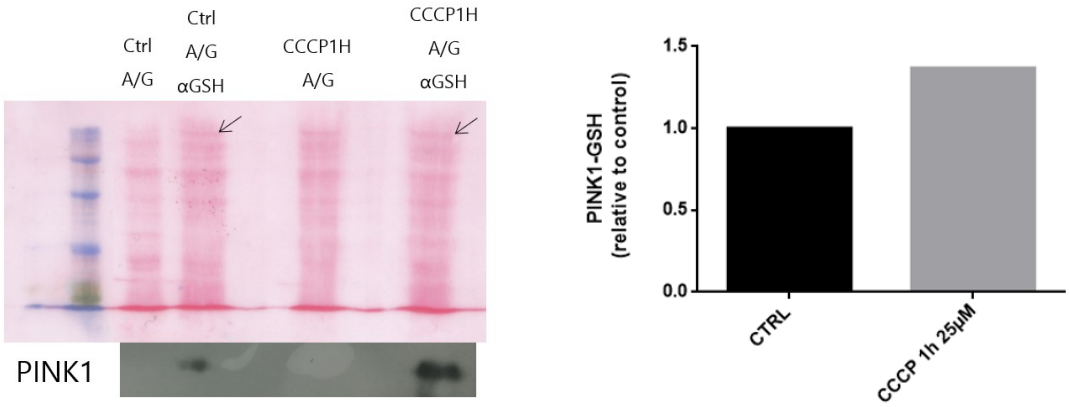


Figure 3.6 **Immunoprecipitation of glutathionylated PINK1**. SH-SY5Y mitoQC cells were treated with or without 25μM CCCP for 1h, followed by mitochondrial fraction isolation. GSH was immunoprecipitated using α-GSH and PINK1 was immunodetected by Western blot, 30 μg of protein were load per well. A) Ponceau staining used for checking total protein loading and for normalization of protein total amount quantification from PINK1 – GSH immunoprecipitation (bands used for total load normalization are indicated by the black arrows) and bands obtained for the different conditions. B) Glutathionylated PINK1 immunoprecipitation levels relative to control. This experiment has been performed once.

Although many clues indicate the role of protein glutathionylation in mitophagy process, further experiments are needed for disclosing whether PINK1 glutathionylation plays a role in mitophagy control.

## 3.5 GCLC expression levels

To further study the role of GSH signaling in mitophagy, we assessed the expression of the rate limiting enzyme for the production of GSH, Glutamate-cysteine ligase (GCL), in particular its catalytic subunit, GCLC. Accordingly, we questioned if CCCP treatment upregulates GCLC and consequently increases the amount of GSH in SH-SY5Y mitoQC cells. We hypothesized that ROS stimulate GCLC expression in order to promote GSH generation, that in turn can stimulate P-Glu.

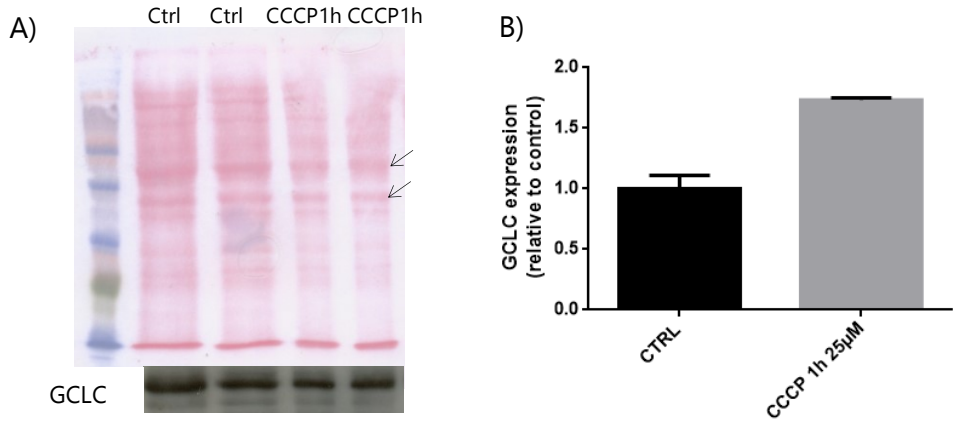


Figure 3.7 **GCLC expression levels**. SH-SY5Y mitoQC cells were treated with 25μM CCCP for 1h or non-treated. Samples recover and western blot performed, 30μl of sample were loaded per well. A) Ponceau staining used for checking total protein loading and for normalization of protein total amount quantification (bands used for total load normalization *per* lane are indicated by the black arrows) and film revelation of GCLC B) GCLC expression values. Values were normalized over control. Representative results show an increase of GCLC levels in cells treated with 25μM CCCP for 1h. Graphs represent the median ± SD of two technical replicates. This experiment was repeated tree times, with similar results.

SH-SY5Y mitoQC cells were treated with and without 25μM of CCCP for 1h, the results (Figure 3.7) show a 60% increase of GCLC expression in CCCP treated cells. Thus, one can speculate that CCCP treatment induces generation of ROS, which act as signaling molecules and enhance GSH production through stimulation of GCLC expression. This would corroborate our hypothesis that augmentation of GSH in the cells can contribute to stimulate glutathionylation of proteins. To confirm that GCLC augmented expression correlates with an increase in GSH levels, quantification of GSH levels in the cells must be done.

## 3.6 GCLC knock down optimization

To validate the importance of GSH and GCLC in mitophagy stimulation, there is the need to inhibit GCLC expression for further assessment of GSH levels and mitophagy rates. Thus, siRNA tools against GCLC were used. In order to optimize the knocking down process, different time-points (24h or 48h) and siRNA-GCLC concentrations (5,10 or 15 pmol *per* well) were used, and GCLC levels of total cell extracts from SH-SY5Y mitoQC were determined by immunoblot.

The results (Figure 3.8) show that 48h treatment with 15 pmol is the most effective one, as it presents a decrease of approximately 30% in GCLC expression in relation to control 48h. To confirm that this silencing is effective GSH levels need to be quantified.

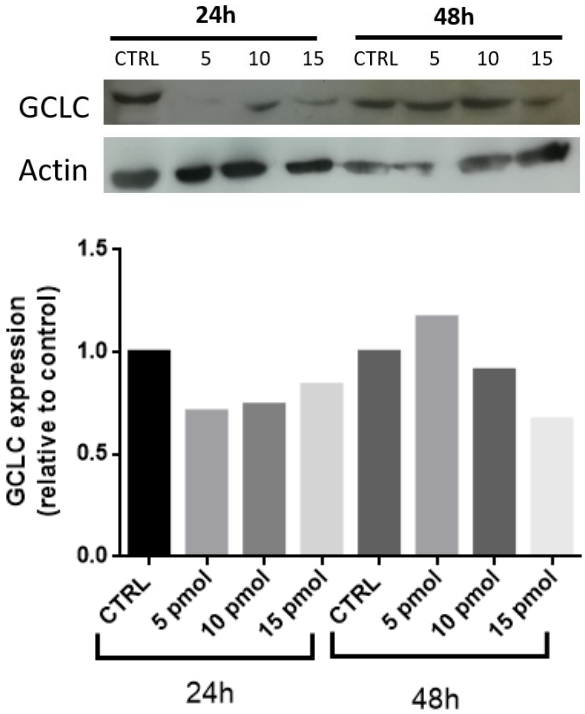


Figure 3.8 **GCLC expression was silenced in SH-SY5Y mitoQC cells**. Cells were treated with 5,10 or 15 pmol of siRNA *per* well for 24h or 48h, samples recover western blot performed, 30µl of sample were loaded per well. Protein values were normalized using actin expression values. GCLC levels presented are relative to controls for each related time point. Representative results of one technical replicate. This experiment was repeated tree times, with similar results.

## 3.7 GSH and GSSG levels quantification

Total glutathione levels (GSH and GSSG) quantification is an important read out to functionally validate that siRNA GCLC treatment did decrease GCLC expression by affecting final GSH levels. Likewise, quantification of cellular GSH during CCCP-induced mitophagy will help to validate our hypothesis that ROS-induced mitophagy occurs by modulating GSH levels and signaling. Thus, GCLC silenced and non-silenced SH-SY5Y mitoQC cells were treated with 25µM CCCP for 1h, samples were recovered, and quantification protocol followed. An example of the expected kinetics variation for similar conditions is presented in Figure 3.9 A).

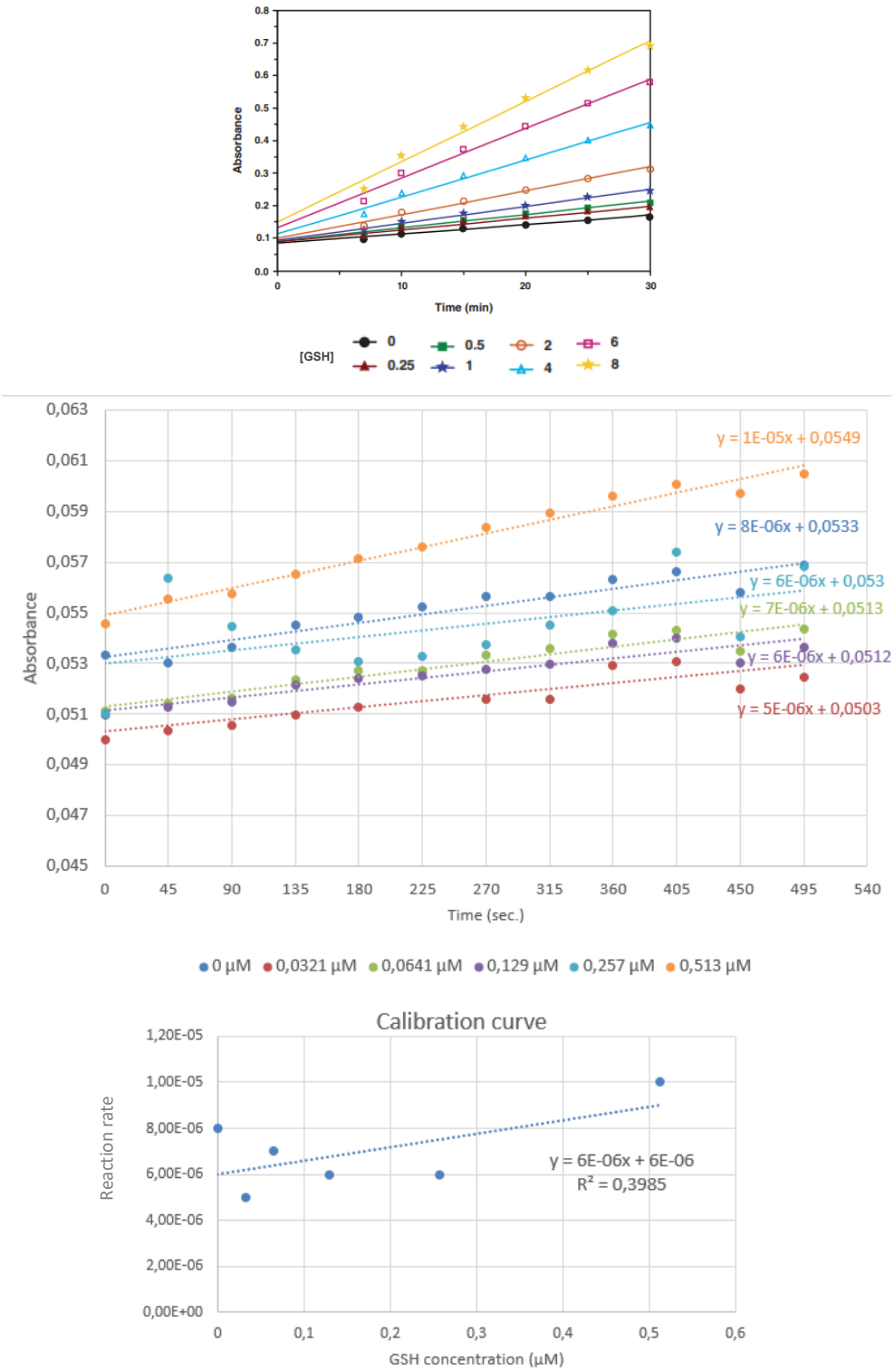


Figure 3.9 **GCLC kinetics and standard curve** A) Example of expected kinetics evolution for different final concentrations of GSH in the samples. Retrieved from Cayman B) Kinetics obtained for standard GSH concentrations (0 µM, 0.0321 µM, 0.0641 µM, 0.129 µM, 0.257 µM and 0.513 µM), the respective linear regression trend lines and equations are presented C) Standard curve obtained from the slopes of the different GSH concentration line equations, the respective equation and $R^2$ are presented.

The results obtained from the quantification protocol for the standard GSH samples are shown in Figure 3.9 B) and C). Unfortunately, the kinetics obtained for the different concentrations of GSH are inconsistent (Figure 3.9 B) ), with samples with 0 μM of GSH having higher absorbance values (corresponding to more GSH present in the sample) than samples with 0,0321 μM, 0,0641 μM and 0,129 μM of GSH. A possible factor that might have contributed for the inconsistent results obtained is the fact that we used an old DTNB reagent.

Still, we used these kinetics to obtained a standard GSH calibration curve. Unfortunately, a $R^2$ value of 0.3985 is too low to use this calibration curve with confidence to obtain GSH levels in the different samples. So, no further results regarding GSH levels within each sample were obtained.

Due to delays in the arriving of the reagents we only had time to perform this experiment a single time, so no conclusive results over GCLC silencing effectiveness, its importance to the overall GSH levels in the cells, and its implication in a successful mitophagy was not possible to respond. Thus, in the future for the continuity of this project, this experiment needs to be repeated to finally respond if whether or not GSH levels are implied in GSH signaling and mitophagy induction/progression.

# 4

# DISCUSSION

Mitochondria are pivotal multipurpose organelles, whose deregulation and damage leads to ROS production and oxidative stress, which may cause cell death or senescence and contribute to onset and progression of diseases such as stroke and neurodegenerative diseases. Being such important elements to keep cell homeostasis, it is imperative to know more about how mitochondria are eliminated and mitochondrial quality control is maintained. Mitophagy is the process by which damage or excessive mitochondria are eliminated. At the same time, mitochondria are the main cellular source of ROS. Under physiological conditions and at low levels, ROS act as signaling molecules, while excessive ROS leads to oxidative stress. ROS are counteracted by GSH, the main non-protein antioxidant within the cells, which decreases the GSH/GSSG ratio and stimulates protein S-glutathionylation, a post translation modification that can change protein function and regulate several cell processes.

In this work we aimed to explore mitophagy and its pathways, in particular whether they are regulated by redox and GSH signaling. The identification of novel players that mediate mitophagy can facilitate the development of new strategies to protect cells and eventually to improve available therapies against oxidative stress and mitochondrial damage occurring in several diseases, including stroke.

We hypothesized that mitophagy can be regulated by GSH signaling. Namely that dysfunctional mitochondria produce ROS that can induce production and oxidation of GSH, which promotes protein S-glutathionylation. Our hypothesis is that glutathionylation can enhance mitophagy by modulating the activity of key mitophagy-related proteins as a redox cytoprotective adaptation, for the elimination of dysfunctional mitochondria.

The classical mitochondrial uncoupler CCCP was used to induce mild mitochondrial ROS production capable of inducing mitophagy without cell death. Thus, mimicking dysfunctional mitochondria that accumulates in the cells with aging or disease.

In this study, two human neuronal cell lines were used SH-SY5Y and SH-SY5Y mitoQC. SH-SY5Y mitoQC cell line has a useful mitophagy reporter, mitoQC, that allows following mitophagy in an accurate manner. In this work we optimize new readouts to measure mitophagy with mitoQC.

Mitophagy is a highly dynamic process that can be difficult to quantify, herein we used confocal microscopy, flow cytometry and, for the first time, a microplate reader to evaluate this MQC process in SH-SY5Y mitoQC cells. By measuring red and green fluorescence, we were able to calculate mitophagy rates and showed that there is possible to use a microplate reader to detect significantly different mitophagy rates between non-treated and CCCP-treated cells. Though, this novel approach is still very undeveloped and needs further optimization. For example, use different time points and concentrations of CCCP and assess mitophagy rates differences. Testing other mitophagy inducers such as Antimycin A (Complex III inhibitor) + Oligomycin (ATP synthase inhibitor), as well as inhibitors of mitophagy such as Ciclosporin A or Bafilomycin, can help microplate readout optimization. As well, at the same time other methods that corroborate the results must be used to validate its worth as a new technique for assessing mitophagy. Nevertheless, we were able to contribute with a new, faster and simpler technique that facilitates the investigation of mitophagy.

Likewise, the use of flow cytometry is a promising technique to measure mitophagy using mitoQC, however our results did not show higher levels of mitophagy in 1h CCCP treated condition. This result is in contrast to our microplate and microscopy result and previous results from our lab and the literature. Nevertheless, is important to note that this experiment was still an optimization for the use of this technique to assess mitophagy and some adjustments might be needed. Besides using lasers with precise wavelengths to stimulate the mitoQC probe, the duration of the CCCP treatment might have to be extended. Indeed, others have shown, using flow cytometry, that CCCP is cable of inducing mitophagy using longer treatments [121,124]. Inclusive, Boya and colleagues were able to show in SH-SY5Y cells using MitoTracker deep red, that CCCP treatment for 6 and 16h induces mitophagy[121]. Another adjustment may be the cellular

confluence used when performing the CCCP treatment, perhaps treating less cells may offer a different result, since with higher confluences cells are more protected from the ionophore.

Finally, confocal microscopy is an accurate technique to assess mitophagy, here we were able to show that CCCP causes the increase of mitolysosomes presence in the cells, thus activating mitophagy. Nonetheless, the evaluation of mitophagy with this method is still a work in progress, as image quantification is time consuming and hard to optimize it needs to keep being improved in the future.

Furthermore, we confirmed the ability of CCCP to induce ROS generation and mitophagy induction through PINK1/ PARKIN pathway in our cell models. In fact, ROS are essential for the progression of the mitophagic process stimulated by CCCP, as the use of ROS scavengers limits the mitophagic process triggered by CCCP treatment[75,116] . As well PINK1 accumulation in the mitochondria proved to be involved in CCCP-induced mitophagy being in agreement with the literature[76].

Herein, the preliminary results obtained suggest that GSH signaling and redox balance are involved in the control of mitophagy, in particular of PINK1/PARKIN mitophagic pathway.

With this work, we were able to show, for the first time, that the mitochondrial kinase PINK1 is glutathionylated when cells are treated with CCCP at low concentrations for mitophagy stimulation. PINK1 acts as a molecular sensor for mitochondrial damage, being essential for maintain mitochondrial quality control [125].Protein S-glutathionylation is stimulated in an oxidative environment in order to protect protein's critic cysteine residues and also as a way to regulate protein function. In the mitochondria, P-Glu seems to work as a negative feedback controller for ROS production, as a several enzymes of Krebs cycle and electron transport chain are inhibited by P-Glu when GSH/GSSG ratio decreases [112]. Yet, we hypothesize that PINK1 is instead activated by P-Glu with the purpose of inducing mitophagy for the elimination of damaged mitochondria that can generate oxidative stress. Another possibility is that S-glutathionylation protects critic cysteines of PINK1 to avoid their irreversible oxidation and consequent protein dysfunction and elimination.

In fact, Lipton and colleagues demonstrated that PINK1 is susceptible to post-translation modifications that are able to modify its function. In concrete, they showed that in hiPSC-Based Parkinson's Disease Models, S-nitrosylation of PINK1, stimulated by nitrosative stress,

inhibits PINK1's kinase activity and decreases PINK1/PARKIN mitophagy. [123]. In addition, other mitochondria-related proteins have already been found to be modified by P-Glu, in particular, the respiratory chain complex I. In the presence of ROS, GSSG augmentation stimulates complex I glutathionylation trough GRX2 activation, which inhibits complex I activity and in turn reduces ROS production, since complex I is one of the main responsible for the leakage of electrons during respiratory chain[126,127].

In the future, other proteins linked to mitophagy should be evaluated for a possible modification of their activity by P-Glu, of major interest would be investigate PARKIN, since it has critic cysteines whose alteration modulates its activity[128] and just as PINK1 is essential for mitophagy. Besides, another interesting point would be studying PINK1 protein S-glutathionylation process itself, if it occurs spontaneously or if it is regulated by enzymatic action, for example by GRX2, who is already known to regulate several Krebs cycle and electron transport chain related enzymes

Nevertheless, there is the need to repeat this experiment and use complementary techniques to confirm PINK1 glutathionylation, for example with mass spectrometry, and if PINK1 is indeed glutathionylated, disclose the critic cysteine residue involved. And to further explore GSH signaling and its involvement in PINK1/PARKIN mitophagy, it should be investigated if indeed glutathionylation of PINK1 enhances PINK1 activity contributing to enhanced mitophagy. Likewise, it also must be evaluated whether in this working model mitophagy protects neurons against cell death, being a cytoprotective strategy.

In order to further characterize the role of GSH signaling in mitophagy the levels of GCLC, the catalytic subunit of the rate limiting enzyme for GSH production, GCL, were measured. We found that GCLC is upregulated in 1h CCCP treated conditions, showing that CCCP is capable of modulating GSH synthesis. The GSH/GSSG system is one of the main cellular antioxidant defenses. GSH levels are regulated, among others, by its synthesis and by its utilization rates. In response to stress, ROS produced by dysfunctional mitochondria act as signaling molecules and induce the expression of different genes in order to suppress this production and to boost antioxidant defense. It has been shown that ROS are able to activate Nrf1 and Nrf2, which by their turn are responsible for activating GCLC promoter and thus inducing GCLC expression which leads to GSH production [129]. This GSH can then be oxidized by ROS, forming

GSSG that can stimulate P-Glu and maybe can signal to enhance mitophagy. Nevertheless, whenever stress is too high generating excessive ROS, cell death can be triggered.

Unfortunately, we could not quantify GSH levels successfully and did not had the time to find if GSH levels are indeed higher when GCLC is upregulated or lower when GCLC is silenced with siRNA. Thus, it was not possible to associate the increased levels of PINK1 glutathionylation with GSH levels and signaling. So, in the future to continue this project GSH quantification must be performed.

Although it was not possible to explore the possible role of mitophagy and P-Glu as cytoprotective processes in stress-related conditions like stroke, it is the objective for future work. As such, for example, to continue this work mitophagy-induced cytoprotection should be tested, first cells should be treated with CCCP to induce mild signaling ROS and stimulate mitophagy, and then cell death should be promoted for example using t-BHP or glutamate (for mimicking stroke related excitotoxicity). Another interesting possibility would be test the influence of N-acetylcysteine, an antioxidant precursor of GSH, in mitophagy, protein S-glutathionylation and cell survival.

In this study, we were able to confirm the previous reports that CCCP is able to induce ROS generation and mitophagy onset through PINK1 stabilization on the OMM. Most relevant, we display protein S-glutathionylation as a possible novel way of regulation of mitophagy through PINK1 glutathionylation induced by ROS signaling.

To know the mechanism behind mitophagy is of the outmost importance as its possible manipulation to promote cytoprotection against ROS generation and stress holds great value in future therapeutic approaches for diseases like stroke.

# 6

# CONCLUSION

Mitophagy is an adaptative and cytoprotective mechanism, essential to eliminate damage or excessive mitochondria that represent a threat to the cells and avoid cell death. Given the importance of mitochondria in oxidative stress related injuries and its potential as therapeutical target, mitophagy pathways and regulation must be explored. Protein S-glutathionylation is an adaptative mechanism capable of regulating protein function involved in regulation of several cellular processes. Herein, we demonstrated that P-Glu has the potential to regulate mitophagy response to mild oxidative stress. Further experiments are needed for a better understanding of P-Glu involvement in mitophagy, namely if PINK1 is the single player or if there are other regulated proteins. Still, whether P-Glu depends only on newly produced GSH and GCLC, or also on GSH recycling and pentose phosphate pathway. Finally, and importantly, if P-Glu mediated mitophagy can be a cytoprotective mechanisms and if it can be stimulated exogenously in order to avoid cell death in a stressful context. By understanding these mechanisms, one can attempt to modulate them to promote cytoprotection and eventually use mitophagy induction as a therapeutic strategy against diseases characterized by mitophagic damage such as stroke.

# REFERENCES


1. Word Health Organization. The top 10 causes of death. https://www.who.int/news-room/fact-sheets/detail/the-top-10-causes-of-death (2020).
2. Kuriakose, D. & Xiao, Z. Pathophysiology and treatment of stroke: Present status and future perspectives. *International Journal of Molecular Sciences* vol. 21 Preprint at https://doi.org/10.3390/ijms21207609 (2020).
3. Campbell, B. C. V. *et al.* Ischaemic stroke. *Nat Rev Dis Primers* **5**, (2019).
4. Mir, M. A., Al-Baradie, R. S. & Alhussainawi, M. D. *Pathophysiology of Strokes*. (2014).
5. Unnithan AKA, M Das J, M. P. Hemorrhagic Stroke. *StatPearls [Internet]. Treasure Island (FL): StatPearls Publishing*.
6. Ames, A. & Nesbett, F. B. Pathophysiology of ischemic cell death: I. Time of onset of irreversible damage; importance of the different components of the ischemic insult. *Stroke* **14**, (1983).
7. Kalogeris, T., Baines, C. P., Krenz, M. & Korthuis, R. J. Cell Biology of Ischemia/Reperfusion Injury. in *International Review of Cell and Molecular Biology* vol. 298 (2012).
8. Theodore Kalogeris, Christopher P. Baines, Maike Krenz, and R. J. K. Ischemia/Reperfusion. *Physiol Behav* **176**, 139–148 (2017).
9. Broughton, B. R. S., Reutens, D. C. & Sobey, C. G. Apoptotic mechanisms after cerebral ischemia. *Stroke* **40**, (2009).
10. Yang, J. L., Mukda, S. & Chen, S. Der. Diverse roles of mitochondria in ischemic stroke. *Redox Biol* **16**, 263–275 (2018).
11. Ginsberg, M. D. The new language of cerebral ischemia. *American Journal of Neuroradiology* **18**, 1435–1445 (1997).

12. Mergenthaler, P., Dirnagl, U. & Meisel, A. Pathophysiology of stroke: Lessons from animal models. *Metab Brain Dis* **19**, 151–167 (2004).
13. Marler, J. R. & et.al. Association of outcome with early stroke treatment: Pooled analysis of ATLANTIS, ECASS, and NINDS rt-PA stroke trials. *Lancet* **363**, (2004).
14. Goyal, M. *et al.* Endovascular thrombectomy after large-vessel ischaemic stroke: A meta-analysis of individual patient data from five randomised trials. *The Lancet* **387**, (2016).
15. Kalogeris, T., Baines, C. P., Krenz, M. & Korthuis, R. J. Ischemia/reperfusion. *Compr Physiol* **7**, 113–170 (2017).
16. Shen, L. *et al.* Mitophagy in Cerebral Ischemia and Ischemia/Reperfusion Injury. *Front Aging Neurosci* **13**, 1–17 (2021).
17. Sanderson, T. H., Reynolds, C. A., Kumar, R., Przyklenk, K. & Hüttemann, M. Molecular mechanisms of ischemia-reperfusion injury in brain: Pivotal role of the mitochondrial membrane potential in reactive oxygen species generation. *Mol Neurobiol* **47**, 9–23 (2013).
18. Kalogeris, T., Bao, Y. & Korthuis, R. J. Mitochondrial reactive oxygen species: A double edged sword in ischemia/reperfusion vs preconditioning. *Redox Biol* **2**, 702–714 (2014).
19. Zhang, X. *et al.* Cerebral ischemia-reperfusion-induced autophagy protects against neuronal injury by mitochondrial clearance. *Autophagy* **9**, 1321–1333 (2013).
20. Galluzzi, L., Kepp, O., Trojel-Hansen, C. & Kroemer, G. Mitochondrial control of cellular life, stress, and death. *Circ Res* **111**, 1198–1207 (2012).
21. Houten, S. M. & Wanders, R. J. A. A general introduction to the biochemistry of mitochondrial fatty acid β-oxidation. *Journal of Inherited Metabolic Disease* vol. 33 Preprint at https://doi.org/10.1007/s10545-010-9061-2 (2010).
22. Ajioka, R. S., Phillips, J. D. & Kushner, J. P. Biosynthesis of heme in mammals. *Biochimica et Biophysica Acta - Molecular Cell Research* vol. 1763 Preprint at https://doi.org/10.1016/j.bbamcr.2006.05.005 (2006).
23. Lill, R. & Mühlenhoff, U. Iron-sulfur-protein biogenesis in eukaryotes. *Trends in Biochemical Sciences* vol. 30 Preprint at https://doi.org/10.1016/j.tibs.2005.01.006 (2005).
24. Li, X. *et al.* Targeting mitochondrial reactive oxygen species as novel therapy for inflammatory diseases and cancers. *J Hematol Oncol* **6**, 1–19 (2013).
25. Li, X. *et al.* Targeting mitochondrial reactive oxygen species as novel therapy for inflammatory diseases and cancers. *J Hematol Oncol* **6**, 1–19 (2013).
26. Venditti, P., Di Stefano, L. & Di Meo, S. Mitochondrial metabolism of reactive oxygen species. *Mitochondrion* **13**, 71–82 (2013).

27. Burdon, R. H., Gill, V. & Rice-Evans, C. Cell proliferation and oxidative stress. *Free Radic Res* **7**, (1989).
28. Sauer, H., Rahimi, G., Hescheler, J. & Wartenberg, M. Role of reactive oxygen species and phosphatidylinositol 3-kinase in cardiomyocyte differentiation of embryonic stem cells. *FEBS Lett* **476**, (2000).
29. Kamata, H. *et al.* Reactive oxygen species promote TNFα-induced death and sustained JNK activation by inhibiting MAP kinase phosphatases. *Cell* **120**, 649–661 (2005).
30. Pickles, S., Vigié, P. & Youle, R. J. Mitophagy and Quality Control Mechanisms in Mitochondrial Maintenance. *Current Biology* **28**, R170–R185 (2018).
31. Yoo, S. M. & Jung, Y. K. A molecular approach to mitophagy and mitochondrial dynamics. *Mol Cells* **41**, 18–26 (2018).
32. Tilokani, L., Nagashima, S., Paupe, V. & Prudent, J. Mitochondrial dynamics: Overview of molecular mechanisms. *Essays in Biochemistry* vol. 62 Preprint at https://doi.org/10.1042/EBC20170104 (2018).
33. Popov, L. D. Mitochondrial biogenesis: An update. *J Cell Mol Med* **24**, 4892–4899 (2020).
34. Ventura-Clapier, R., Garnier, A. & Veksler, V. Transcriptional control of mitochondrial biogenesis: The central role of PGC-1α. *Cardiovascular Research* vol. 79 Preprint at https://doi.org/10.1093/cvr/cvn098 (2008).
35. Steiner, J. L., Murphy, E. A., McClellan, J. L., Carmichael, M. D. & Davis, J. M. Exercise training increases mitochondrial biogenesis in the brain. *J Appl Physiol* **111**, (2011).
36. Klingenspor, M. Cold-induced recruitment of brown adipose tissue thermogenesis. *Experimental Physiology* vol. 88 Preprint at https://doi.org/10.1113/eph8802508 (2003).
37. Gutsaeva, D. R. *et al.* Transient hypoxia stimulates mitochondrial biogenesis in brain subcortex by a neuronal nitric oxide synthase-dependent mechanism. *Journal of Neuroscience* **28**, (2008).
38. Zhu, L. *et al.* Hypoxia induces PGC-1α expression and mitochondrial biogenesis in the myocardium of TOF patients. *Cell Res* **20**, (2010).
39. Wu, Z. *et al.* Mechanisms controlling mitochondrial biogenesis and respiration through the thermogenic coactivator PGC-1. *Cell* **98**, (1999).
40. Handschin, C. & Spiegelman, B. M. Peroxisome proliferator-activated receptor γ coactivator 1 coactivators, energy homeostasis, and metabolism. *Endocr Rev* **27**, (2006).
41. Shao, D. *et al.* PGC-1β-Regulated mitochondrial biogenesis and function in myotubes is mediated by NRF-1 and ERRα. *Mitochondrion* **10**, (2010).

42. Twig, G. *et al.* Fission and selective fusion govern mitochondrial segregation and elimination by autophagy. *EMBO Journal* **27**, (2008).
43. Frank, M. *et al.* Mitophagy is triggered by mild oxidative stress in a mitochondrial fission dependent manner. *Biochim Biophys Acta Mol Cell Res* **1823**, 2297–2310 (2012).
44. Nakada, K. *et al.* Inter-mitochondrial complementation: Mitochondria-specific system preventing mice from expression of disease phenotypes by mutant mtDNA. *Nat Med* **7**, (2001).
45. Youle, R. J. & Van Der Bliek, A. M. Mitochondrial fission, fusion, and stress. *Science* vol. 337 Preprint at https://doi.org/10.1126/science.1219855 (2012).
46. Song, Z., Ghochani, M., McCaffery, J. M., Frey, T. G. & Chan, D. C. Mitofusins and OPA1 mediate sequential steps in mitochondrial membrane fusion. *Mol Biol Cell* **20**, (2009).
47. Leduc-Gaudet, J. P., Hussain, S. N. A., Barreiro, E. & Gouspillou, G. Mitochondrial dynamics and mitophagy in skeletal muscle health and aging. *International Journal of Molecular Sciences* vol. 22 Preprint at https://doi.org/10.3390/ijms22158179 (2021).
48. Youle, R. J. & Narendra, D. P. Mechanisms of mitophagy. *Nat Rev Mol Cell Biol* **12**, (2011).
49. Kaur, J. & Debnath, J. Autophagy at the crossroads of catabolism and anabolism. *Nat Rev Mol Cell Biol* **16**, 461–472 (2015).
50. Glick, D., Barth, S. & Macleod, K. F. Autophagy: Cellular and molecular mechanisms. *Journal of Pathology* vol. 221 Preprint at https://doi.org/10.1002/path.2697 (2010).
51. Feng, Y., He, D., Yao, Z. & Klionsky, D. J. The machinery of macroautophagy. *Cell Res* **24**, 24–41 (2014).
52. Hansen, M., Rubinsztein, D. C. & Walker, D. W. Autophagy as a promoter of longevity: insights from model organisms. *Nat Rev Mol Cell Biol* **19**, 579–593 (2018).
53. Doxaki, C. & Palikaras, K. Neuronal Mitophagy: Friend or Foe? *Frontiers in Cell and Developmental Biology* vol. 8 Preprint at https://doi.org/10.3389/fcell.2020.611938 (2021).
54. Valente, E. M. *et al.* Hereditary Early-Onset Parkinson's Disease Caused by Mutations in <em>PINK1</em> *Science (1979)* **304**, (2004).
55. Kerr, J. S. *et al.* Mitophagy and Alzheimer's Disease: Cellular and Molecular Mechanisms. *Trends in Neurosciences* vol. 40 Preprint at https://doi.org/10.1016/j.tins.2017.01.002 (2017).
56. De Gaetano, A. *et al.* Mitophagy and oxidative stress: The role of aging. *Antioxidants* **10**, 1–25 (2021).
57. Palikaras, K., Lionaki, E. & Tavernarakis, N. Mechanisms of mitophagy in cellular homeostasis, physiology and pathology. *Nat Cell Biol* **20**, 1013–1022 (2018).

58. Valente, E. M. *et al.* Hereditary early-onset Parkinson's disease caused by mutations in PINK1. *Science (1979)* **304**, (2004).
59. Lan, R. *et al.* Mitophagy is activated in brain damage induced by cerebral ischemia and reperfusion via the PINK1/Parkin/p62 signalling pathway. *Brain Res Bull* **142**, (2018).
60. Narendra, D., Tanaka, A., Suen, D. F. & Youle, R. J. Parkin is recruited selectively to impaired mitochondria and promotes their autophagy. *Journal of Cell Biology* **183**, (2008).
61. Meissner, C., Lorenz, H., Weihofen, A., Selkoe, D. J. & Lemberg, M. K. The mitochondrial intramembrane protease PARL cleaves human Pink1 to regulate Pink1 trafficking. *J Neurochem* **117**, (2011).
62. Jin, S. M. *et al.* Mitochondrial membrane potential regulates PINK1 import and proteolytic destabilization by PARL. *Journal of Cell Biology* **191**, (2010).
63. Yamano, K. & Youle, R. J. PINK1 is degraded through the N-end rule pathway. *Autophagy* **9**, (2013).
64. Lazarou, M., Jin, S. M., Kane, L. A. & Youle, R. J. Role of PINK1 Binding to the TOM Complex and Alternate Intracellular Membranes in Recruitment and Activation of the E3 Ligase Parkin. *Dev Cell* **22**, (2012).
65. Okatsu, K. *et al.* PINK1 autophosphorylation upon membrane potential dissipation is essential for Parkin recruitment to damaged mitochondria. *Nat Commun* **3**, 1010–1016 (2012).
66. Okatsu, K. *et al.* A dimeric pink1-containing complex on depolarized mitochondria stimulates parkin recruitment. *Journal of Biological Chemistry* **288**, (2013).
67. Koyano, F. *et al.* Ubiquitin is phosphorylated by PINK1 to activate parkin. *Nature* **510**, (2014).
68. Kondapalli, C. *et al.* PINK1 is activated by mitochondrial membrane potential depolarization and stimulates Parkin E3 ligase activity by phosphorylating Serine 65. *Open Biol* **2**, (2012).
69. Sauvé, V. *et al.* A Ubl/ubiquitin switch in the activation of Parkin. *EMBO J* **34**, (2015).
70. Gegg, M. E. *et al.* Mitofusin 1 and mitofusin 2 are ubiquitinated in a PINK1/parkin-dependent manner upon induction of mitophagy. *Hum Mol Genet* **19**, (2010).
71. Geisler, S. *et al.* PINK1/Parkin-mediated mitophagy is dependent on VDAC1 and p62/SQSTM1. *Nat Cell Biol* **12**, 119–131 (2010).
72. Chan, N. C. *et al.* Broad activation of the ubiquitin-proteasome system by Parkin is critical for mitophagy. *Hum Mol Genet* **20**, (2011).

73. Wong, Y. C. & Holzbaur, E. L. F. Optineurin is an autophagy receptor for damaged mitochondria in parkin-mediated mitophagy that is disrupted by an ALS-linked mutation. *Proc Natl Acad Sci U S A* **111**, (2014).
74. No Title. https://www.biolegend.com/en-us/bio-bits/pink1-mediated-activation-and-recruitment-of-parkin-to-the-mitochondria.
75. Xiao, B. *et al.* Reactive oxygen species trigger Parkin/PINK1 pathway–dependent mitophagy by inducing mitochondrial recruitment of Parkin. *Journal of Biological Chemistry* **292**, 16697–16708 (2017).
76. Gómez-Sánchez, R. *et al.* Mitochondrial impairment increases FL-PINK1 levels by calcium-dependent gene expression. *Neurobiol Dis* **62**, 426–440 (2014).
77. Birgisdottir, Å. B., Lamark, T. & Johansen, T. The LIR motif - crucial for selective autophagy. *Journal of Cell Science* vol. 126 Preprint at https://doi.org/10.1242/jcs.126128 (2013).
78. Chen, G. *et al.* A regulatory signaling loop comprising the PGAM5 phosphatase and CK2 controls receptor-mediated mitophagy. *Mol Cell* **54**, (2014).
79. Liu, L. *et al.* Mitochondrial outer-membrane protein FUNDC1 mediates hypoxia-induced mitophagy in mammalian cells. *Nat Cell Biol* **14**, (2012).
80. Wu, W. *et al.* ULK1 translocates to mitochondria and phosphorylates FUNDC1 to regulate mitophagy. *EMBO Rep* **15**, (2014).
81. Matsushima, M. *et al.* Isolation, mapping, and functional analysis of a novel human cDNA (BNIP3L) encoding a protein homologous to human NIP3. *Genes Chromosomes Cancer* **21**, (1998).
82. Li, Y. *et al.* BNIP3L/NIX-mediated mitophagy: molecular mechanisms and implications for human disease. *Cell Death and Disease* vol. 13 Preprint at https://doi.org/10.1038/s41419-021-04469-y (2022).
83. Sandoval, H. *et al.* Essential role for Nix in autophagic maturation of erythroid cells. *Nature* **454**, (2008).
84. Birben, E., Sahiner, U. M., Sackesen, C., Erzurum, S. & Kalayci, O. Oxidative stress and antioxidant defense. *World Allergy Organization Journal* **5**, 9–19 (2012).
85. Morales, A., Colell, A. & Ferna, C. Mitochondrial Glutathione, a Key Survival Antioxidant Montserrat. **11**, (2009).
86. Matsui, R. *et al.* Redox Regulation via Glutaredoxin-1 and Protein S-Glutathionylation. *Antioxid Redox Signal* **32**, 677–700 (2020).

87. Marí, M. *et al.* Mitochondrial glutathione: Recent insights and role in disease. *Antioxidants* **9**, 1–21 (2020).
88. Forman, H. J., Zhang, H. & Rinna, A. Glutathione: Overview of its protective roles, measurement, and biosynthesis. *Mol Aspects Med* **30**, 1–12 (2009).
89. Ribas, V., García-Ruiz, C. & Fernández-Checa, J. C. Glutathione and mitochondria. *Front Pharmacol* **5 JUL**, 1–19 (2014).
90. Aquilano, K., Baldelli, S. & Ciriolo, M. R. Glutathione: New roles in redox signalling for an old antioxidant. *Front Pharmacol* **5 AUG**, 1–12 (2014).
91. Ei Soon Cho, Sahyoun, N. & Stegink, L. D. Tissue glutathione as a cyst(e)ine reservoir during fasting and refeeding of rats. *Journal of Nutrition* **111**, (1981).
92. Lu, S. C. Regulation of glutathione synthesis. *Molecular Aspects of Medicine* vol. 30 Preprint at https://doi.org/10.1016/j.mam.2008.05.005 (2009).
93. Sipos, K. *et al.* Maturation of cytosolic iron-sulfur proteins requires glutathione. *Journal of Biological Chemistry* **277**, (2002).
94. Poot, M., Teubert, H., Rabinovitch, P. S. & Kavanagh, T. J. De novo synthesis of glutathione is required for both entry into and progression through the cell cycle. *J Cell Physiol* **163**, (1995).
95. Lu, S. C. Glutathione synthesis. *Biochimica et Biophysica Acta - General Subjects* vol. 1830 Preprint at https://doi.org/10.1016/j.bbagen.2012.09.008 (2013).
96. Meister, A. & Anderson, M. E. Glutathione. *Annu Rev Biochem* **Vol. 52**, (1983).
97. Chen, Y., Shertzer, H. G., Schneider, S. N., Nebert, D. W. & Dalton, T. P. Glutamate cysteine ligase catalysis: Dependence on ATP and modifier subunit for regulation of tissue glutathione levels. *Journal of Biological Chemistry* **280**, (2005).
98. Ravuri, C., Svineng, G. & Huseby, N. E. Differential regulation of γ-glutamyltransferase and glutamate cysteine ligase expression after mitochondrial uncoupling: γ- glutamyltransferase is regulated in an Nrf2- and NFκB-independent manner. *Free Radic Res* **47**, 394–403 (2013).
99. Yang, H., Magilnick, N., Ou, X. & Lu, S. C. Tumour necrosis factor α induces co-ordinated activation of rat GSH synthetic enzymes via nuclear factor κB and activator protein-1. *Biochemical Journal* **391**, (2005).
100. Calabrese, G., Morgan, B. & Riemer, J. Mitochondrial Glutathione: Regulation and Functions. *Antioxid Redox Signal* **27**, 1162–1177 (2017).
101. Calabrese, G., Morgan, B. & Riemer, J. Mitochondrial Glutathione: Regulation and Functions. *Antioxid Redox Signal* **27**, 1162–1177 (2017).

102. Editors, G., Cadenas, E., Davies, K. J. A. & Adenas, E. N. C. MITOCHONDRIAL FREE RADICAL GENERATION, OXIDATIVE STRESS, AND AGING. *Free Radic Biol Med* **29**, 201–383 (2000).
103. Ribas, V., García-Ruiz, C. & Fernández-Checa, J. C. Glutathione and mitochondria. *Front Pharmacol* **5 JUL**, 1–19 (2014).
104. Dalle-Donne, I. *et al.* Molecular mechanisms and potential clinical significance of S-glutathionylation. *Antioxid Redox Signal* **10**, 445–473 (2008).
105. Homolya, L., Váradi, A. & Sarkadi, B. Multidrug resistance-associated proteins: Export pumps for conjugates with glutathione, glucuronate or sulfate. in *BioFactors* vol. 17 (2003).
106. Gu, F., Chauhan, V. & Chauhan, A. Glutathione redox imbalance in brain disorders. *Current Opinion in Clinical Nutrition and Metabolic Care* vol. 18 Preprint at https://doi.org/10.1097/MCO.0000000000000134 (2015).
107. Hill, B. G. & Bhatnagar, A. Protein S-glutathiolation: Redox-sensitive regulation of protein function. *J Mol Cell Cardiol* **52**, 559–567 (2012).
108. Dalle-Donne, I., Rossi, R., Colombo, G., Giustarini, D. & Milzani, A. Protein S-glutathionylation: a regulatory device from bacteria to humans. *Trends Biochem Sci* **34**, 85–96 (2009).
109. Mailloux, R. J. & Treberg, J. R. Protein S-glutathionlyation links energy metabolism to redox signaling in mitochondria. *Redox Biol* **8**, 110–118 (2016).
110. Giustarini, D. *et al.* Assessment of glutathione/glutathione disulphide ratio and S-glutathionylated proteins in human blood, solid tissues, and cultured cells. *Free Radical Biology and Medicine* vol. 112 360–375 Preprint at https://doi.org/10.1016/j.freeradbiomed.2017.08.008 (2017).
111. Xiong, Y., Uys, J. D., Tew, K. D. & Townsend, D. M. S-Glutathionylation: From molecular mechanisms to health outcomes. *Antioxid Redox Signal* **15**, 233–270 (2011).
112. Mailloux, R. J. Protein S-glutathionylation reactions as a global inhibitor of cell metabolism for the desensitization of hydrogen peroxide signals. *Redox Biol* **32**, 101472 (2020).
113. Queiroga, C. S. F. *et al.* Glutathionylation of adenine nucleotide translocase induced by carbon monoxide prevents mitochondrial membrane permeabilization and apoptosis. *Journal of Biological Chemistry* **285**, 17077–17088 (2010).
114. Mohr, S., Hallak, H., De Boitte, A., Lapetina, E. G. & Brüne, B. Nitric oxide-induced S-glutathionylation and inactivation of glyceraldehyde-3-phosphate dehydrogenase. *Journal of Biological Chemistry* **274**, (1999).

115. Cha, S. J., Kim, H., Choi, H. J., Lee, S. & Kim, K. Protein Glutathionylation in the Pathogenesis of Neurodegenerative Diseases. *Oxid Med Cell Longev* **2017**, (2017).
116. Xiao, B. *et al.* Superoxide drives progression of Parkin/PINK1-dependent mitophagy following translocation of Parkin to mitochondria. *Cell Death Dis* **8**, 1–12 (2017).
117. Park, Y. S., Choi, S. E. & Koh, H. C. PGAM5 regulates PINK1/Parkin-mediated mitophagy via DRP1 in CCCP-induced mitochondrial dysfunction. *Toxicol Lett* **284**, (2018).
118. McWilliams, T. G. & Ganley, I. G. Investigating mitophagy and mitochondrial morphology in vivo using mito-QC: A comprehensive guide. in *Methods in Molecular Biology* vol. 1880 (2019).
119. Joselin, A. P. *et al.* ROS-dependent regulation of parkin and DJ-1 localization during oxidative stress in neurons. *Hum Mol Genet* **21**, (2012).
120. Yang, J. H., Gross, R. L., Basinger, S. F. & Wu, S. M. Apoptotic cell death of cultured salamander photoreceptors induced by cccp: CsA-insensitive mitochondrial permeability transition. *J Cell Sci* **114**, (2001).
121. Mauro-Lizcano, M. *et al.* New method to assess mitophagy flux by flow cytometry. *Autophagy* **11**, (2015).
122. Lazarou, M. *et al.* The ubiquitin kinase PINK1 recruits autophagy receptors to induce mitophagy. *Nature* **524**, 309–314 (2015).
123. Oh, C. K. *et al.* S-Nitrosylation of PINK1 Attenuates PINK1/Parkin-Dependent Mitophagy in hiPSC-Based Parkinson's Disease Models. *Cell Rep* **21**, (2017).
124. Um, J. H., Kim, Y. Y., Finkel, T. & Yun, J. Sensitive measurement of mitophagy by flow cytometry using the pH-dependent fluorescent reporter mt-Keima. *Journal of Visualized Experiments* **2018**, (2018).
125. Bayne, A. N. & Trempe, J. F. Mechanisms of PINK1, ubiquitin and Parkin interactions in mitochondrial quality control and beyond. *Cellular and Molecular Life Sciences* **76**, 4589–4611 (2019).
126. Beer, S. M. *et al.* Glutaredoxin 2 catalyzes the reversible oxidation and glutathionylation of mitochondrial membrane thiol proteins: Implications for mitochondrial redox regulation and antioxidant defense. *Journal of Biological Chemistry* **279**, (2004).
127. Gill, R. M., O'Brien, M., Young, A., Gardiner, D. & Mailloux, R. J. Protein S-glutathionylation lowers superoxide/hydrogen peroxide release from skeletal muscle mitochondria through modification of complex I and inhibition of pyruvate uptake. *PLoS One* **13**, (2018).

128. Trempe, J. F. & Fon, E. A. Structure and function of Parkin, PINK1, and DJ-1, the three musketeers of neuroprotection. *Front Neurol* **4 APR**, (2013).
129. Yang, H. *et al.* Nrf1 and Nrf2 Regulate Rat Glutamate-Cysteine Ligase Catalytic Subunit Transcription Indirectly via NF-κB and AP-1. *Mol Cell Biol* **25**, (2005).
130. Allen, G. F. G., Toth, R., James, J. & Ganley, I. G. Loss of iron triggers PINK1/Parkin-independent mitophagy. *EMBO Rep* **14**, 1127–1135 (2013).

# A

# SUPPLEMENTARY IMAGES

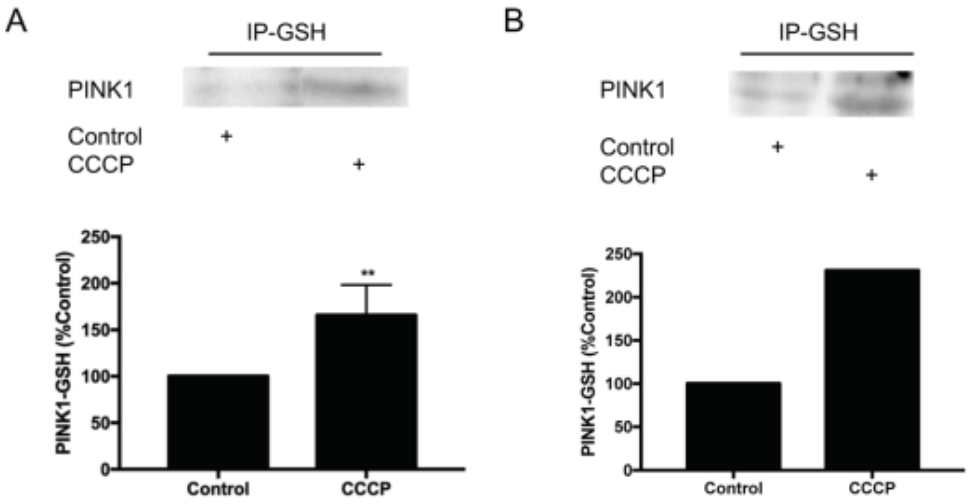


Figure A.1 **CCCP promotes PINK1 and gluthionylation**; A) Purified mitochondria from adult mouse brains were treated with or without CCCP at 25μM for 1h. GSH was immunoprecipitated and PINK1 immunodetected by Western blot. Graphs represent the median ± SD of three experiments. ** p<0,1, compared with the control (PINK1-GSH). B) Primary cultures of astrocytes were treated with or without CCCP at 25μM for 1h, followed by mitochondria isolation; GSH was immunoprecipitated and PINK1 immunodetected by Western blot. This experiment has been repeated two times, with similar results. Adapted from PhD thesis from Cláudia Figueiredo Pereira.

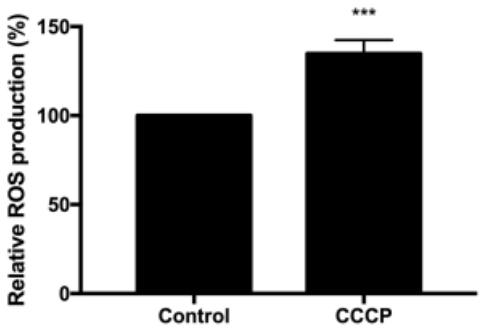


Figure A.2 **CCCP-induced ROS generation**; Quantification of intracellular ROS in primary culture of astrocytes after 1h 25 µM of CCCP treatment, ROS quantification was performed using MitoSOX Red fluorescence dye. Graphs represent the median ± SD of three experiments performed in triplicate. *** p <0.001 compared to control treatment. Adapted from PhD thesis from Cláudia Figueiredo Pereira.

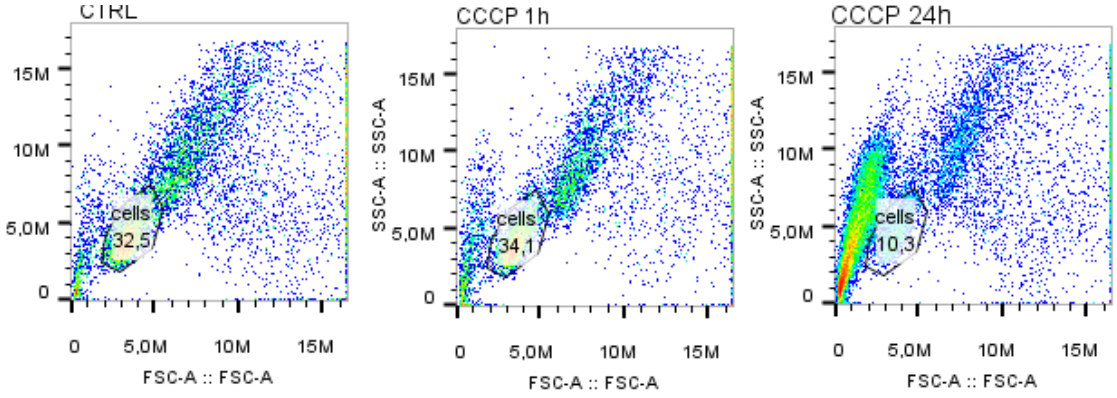


Figure A.3 **SSC vs FSC density plot profile differences between the different conditions: Control; 25 µM CCCP 1h treatment ;10 µM CCCP 24h treatment.**